17. van Boekel, M. A., Vossenaar, E. R., van den Hoogen, F. H. & van Venrooij, W. J. Autoantibody systems in rheumatoid arthritis: specificity, sensitivity and diagnostic value. *Arthritis Res.* **4,** 87–93 (2002).
18. Suzuki, A. *et al.* Functional haplotypes of PADI4, encoding citrullinating enzyme peptidylarginine deiminase 4, are associated with rheumatoid arthritis. *Nat. Genet.* **34,** 395–402 (2003).
19. Wang, Y. *et al.* Human PAD4 regulates histone arginine methylation levels via demethylimination. *Science* **306,** 279–283 (2004).
20. Cuthbert, G. L. *et al.* Histone deimination antagonizes arginine methylation. *Cell* **118,** 545–553 (2004).
21. Martic, G. *et al.* Parathymosin affects the binding of linker histone H1 to nucleosomes and remodels chromatin structure. *J. Biol. Chem.* **280,** 16143–16150 (2005).
22. Li, P. *et al.* PAD4 is essential for antibacterial innate immunity mediated by neutrophil extracellular traps. *J. Exp. Med.* **207,** 1853–1862 (2010).
23. Arita, K. *et al.* Structural basis for Ca(2+)-induced activation of human PAD4. *Nat. Struct. Mol. Biol.* **11,** 777–783 (2004).
24. Top, B. *et al.* Comparative analysis of p53 gene mutations and protein accumulation in human non-small-cell lung cancer. *Int. J. Cancer* **64,** 83–91 (1995).
25. Bodner, S. M. *et al.* Expression of mutant p53 proteins in lung cancer correlates with the class of p53 gene mutation. *Oncogene* **7,** 743–749 (1992).
26. Jones, P. A. & Baylin, S. B. The epigenomics of cancer. *Cell* **128,** 683–692 (2007).
27. Hollstein, M. *et al.* Database of p53 gene somatic mutations in human tumors and cell lines. *Nucleic Acids Res.* **22,** 3551–3555 (1994).
28. Soussi, T. *et al.* Meta-analysis of the p53 mutation database for mutant p53 biological activity reveals a methodologic bias in mutation detection. *Clin. Cancer Res.* **12,** 62–69 (2006).
29. Beroud, C. & Soussi, T. The UMD-p53 database: new mutations and analysis tools. *Hum. Mutat.* **21,** 176–181 (2003).
30. Jenuwein, T. & Allis, C. D. Translating the histone code. *Science* **293,** 1074–80 (2001).
31. Celeste, A. *et al.* H2AX haploinsufficiency modifies genomic stability and tumor susceptibility. *Cell* **114,** 371–383 (2003).
32. Bassing, C. H. *et al.* Histone H2AX: a dosage-dependent suppressor of oncogenic translocations and tumors. *Cell* **114,** 359–370 (2003).
33. Cheung, W. L. *et al.* Apoptotic phosphorylation of histone H2B is mediated by mammalian sterile twenty kinase. *Cell* **113,** 507–517 (2003).
34. Kouzarides, T. Chromatin modifications and their function. *Cell* **128,** 693–705 (2007).
35. Gyorgy, B., Toth, E., Tarcsa, E., Falus, A. & Buzas, E. I. Citrullination: a posttranslational modification in health and disease. *Int. J. Biochem. Cell Biol.* **38,** 1662–1677 (2006).
36. Li, P. *et al.* Regulation of p53 target gene expression by peptidylarginine deiminase 4. *Mol. Cell. Biol.* **28,** 4745–4758 (2008).
37. Chang, X. *et al.* Increased PADI4 expression in blood and tissues of patients with malignant tumors. *BMC Cancer* **9,** 40 (2009).
38. Brown, N. S. & Bicknell, R. Hypoxia and oxidative stress in breast cancer. Oxidative stress: its effects on the growth, metastatic potential and response to therapy of breast cancer. *Breast Cancer Res.* **3,** 323–327 (2001).
39. Toyokuni, S., Okamoto, K., Yodoi, J. & Hiai, H. Persistent oxidative stress in cancer. *FEBS Lett.* **358,** 1–3 (1995).
40. Arita, K. *et al.* Structural basis for histone N-terminal recognition by human peptidylarginine deiminase 4. *Proc. Natl Acad. Sci. USA* **103,** 5291–5296 (2006).
41. Allfrey, V. G. Structural modifications of histones and their possible role in the regulation of ribonucleic acid synthesis. *Proc. Can. Cancer Conf.* **6,** 313–335 (1966).
42. Denis, H. *et al.* Functional connection between deimination and deacetylation of histones. *Mol. Cell Biol.* **29,** 4982–4993 (2009).
43. Li, P. *et al.* Coordination of PAD4 and HDAC2 in the regulation of p53-target gene expression. *Oncogene* **29,** 3153–3162 (2010).
44. Tsukada, T. *et al.* Enhanced proliferative potential in culture of cells from p53-deficient mice. *Oncogene* **8,** 3313–3322 (1993).
45. Shechter, D., Dormann, H. L., Allis, C. D. & Hake, S. B. Extraction, purification and analysis of histones. *Nat. Protoc.* **2,** 1445–1457 (2007).
46. Kato, T. *et al.* Activation of placenta-specific transcription factor distal-less homeobox 5 predicts clinical outcome in primary lung cancer patients. *Clin. Cancer Res.* **14,** 2363–2370 (2008).
47. Kashiwagi, K., Nimura, K., Ura, K. & Kaneda, Y. DNA methyltransferase 3b preferentially associates with condensed chromatin. *Nucleic Acids Res.* **39,** 874–888 (2011).

Acknowledgements

We thank H. Fujiwara for technical assistance. We thank Dr Nobuaki Yoshida and Dr. Toyomasa Katagiri for helpful discussion. This work was supported partially by grant from Japan Society for the Promotion of Science and Ministry of Education, Culture, Sports, Science and Technology of Japan to K.M. and C.T.; grant from Shiseido to C.T.; and Grant-in-Aid from the Tokyo Biochemical Research Foundation to K.M.

Author contributions

C.T., Y.N. and K.M. conceived the project and planned experiments and analyses, which were performed by C.T., M.E. conducted the mutation analysis. K.U. conducted mass analysis. A.S. and K.Y. provided the *Padi4*$^{-/-}$ mice. K.Mas., E.T. and Y.D. conducted tissue microarray analysis. C.T. summarized the whole results. C.T., K.M. and Y.N. wrote the manuscript.

Additional information

Supplementary Information accompanies this paper at http://www.nature.com/naturecommunications

Competing financial interests: The authors declare no competing financial interests.

Reprints and permission information is available online at http://npg.nature.com/reprintsandpermissions/

How to cite this article: Tanikawa, C. *et al.* Regulation of histone modification and chromatin structure by the p53–PADI4 pathway. *Nat. Commun.* 3:676 doi: 10.1038/ncomms1676 (2012).

Published OnlineFirst May 3, 2012; DOI:10.1158/0008-5472.CAN-11-3701

Cancer Research

Histone Lysine Methyltransferase SETD8 Promotes Carcinogenesis by Deregulating PCNA Expression

Masashi Takawa, Hyun-Soo Cho, Shinya Hayami, et al.

Cancer Res 2012;72:3217-3227. Published OnlineFirst May 3, 2012.

Published OnlineFirst May 3, 2012; DOI:10.1158/0008-5472.CAN-11-3701

Molecular and Cellular Pathobiology

Cancer Research

Histone Lysine Methyltransferase SETD8 Promotes Carcinogenesis by Deregulating PCNA Expression

Masashi Takawa[1,3], Hyun-Soo Cho[1], Shinya Hayami[1], Gouji Toyokawa[1], Masaharu Kogure[1,3], Yuka Yamane[1], Yukiko Iwai[1], Kazuhiro Maejima[1], Koji Ueda[2], Akiko Masuda[5], Naoshi Dohmae[5], Helen I. Field[7], Tatsuhiko Tsunoda[6], Takaaki Kobayashi[3], Takayuki Akasu[4], Masanori Sugiyama[3], Shin-ichi Ohnuma[9], Yutaka Atomi[3], Bruce A.J. Ponder[8], Yusuke Nakamura[1,10], and Ryuji Hamamoto[1,8]

Abstract

Although the physiologic significance of lysine methylation of histones is well known, whether lysine methylation plays a role in the regulation of nonhistone proteins has not yet been examined. The histone lysine methyltransferase SETD8 is overexpressed in various types of cancer and seems to play a crucial role in S-phase progression. Here, we show that SETD8 regulates the function of proliferating cell nuclear antigen (PCNA) protein through lysine methylation. We found that SETD8 methylated PCNA on lysine 248, and either depletion of SETD8 or substitution of lysine 248 destabilized PCNA expression. Mechanistically, lysine methylation significantly enhanced the interaction between PCNA and the flap endonuclease FEN1. Loss of PCNA methylation retarded the maturation of Okazaki fragments, slowed DNA replication, and induced DNA damage, and cells expressing a methylation-inactive PCNA mutant were more susceptible to DNA damage. An increase of methylated PCNA was found in cancer cells, and the expression levels of SETD8 and PCNA were correlated in cancer tissue samples. Together, our findings reveal a function for lysine methylation on a nonhistone protein and suggest that aberrant lysine methylation of PCNA may play a role in human carcinogenesis. *Cancer Res; 72(13); 3217–27. ©2012 AACR.*

Introduction

Protein methylation is recently considered an important posttranslational modification and is predominantly found on lysine and arginine residues. Lysine methylation involves the addition of 1 to 3 methyl groups on the amino acid's ε-amine group, to form mono-, di-, or tri-methyllysine. Its function is best understood in histones (1). With the exception of Dot1/DOT1L, all histone lysine methyltransferases (HKMT) contain a SET domain of about 130 amino acids, and so far nearly 40 SET domain–containing HKMTs or potential HKMTs have been identified (2). While our knowledge of the physiologic functions of HKMTs is growing, their involvement in human diseases including cancer is still not well understood.

Proliferating cell nuclear antigen (PCNA) is an evolutionally well-conserved protein found in all eukaryotic species from yeast to humans, as well as in archaea. PCNA functions are related to vital cellular processes such as DNA replication, chromatin remodeling, DNA repair, sister chromatid cohesion, and cell-cycle control (3). PCNA was originally reported as an antigen for autoimmune disease in patients with systemic lupus erythematosus, detected only in the proliferating cell populations (4). Thereafter, it was shown that expression levels of PCNA during cell cycle are differential and associated with proliferation and transformation (5, 6). In the following years, a number of experiments have been done to uncover the role of PCNA in DNA replication, and one of the first functions clarified was a sliding clamp for DNA polymerase δ (7, 8). Meanwhile, the progress in the field not only strengthened the importance of PCNA, but also even placed PCNA at the crossroad of many essential pathways. Importantly, PCNA is posttranslationally modified in several ways, which affects its function. So far, it has been reported that PCNA is ubiquitinated, phosphorylated, acetylated, and even SUMOylated (3). One of the well-documented posttranslational modifications of PCNA is ubiquitination. In response to DNA damage, PCNA is monoubiquitinated at the lysine 164 residue by the E2 Ub–conjugated enzyme Rad6 and the E3 Ub ligase Rad18 (Rad6/Rad18 complex; ref. 9). Rad18 not only binds to Rad6 and PCNA, but also to DNA (10). Thus, Rad18 recruits the ubiquitination machinery to the chromatin-bound target, PCNA. In addition

Authors' Affiliations: [1]Laboratory of Molecular Medicine, Human Genome Center, Institute of Medical Science, The University of Tokyo; [2]Laboratory for Biomarker Development, RIKEN, Minato-ku; [3]Department of Surgery, Kyorin University School of Medicine, Mitaka; [4]Division of Colorectal Surgery, National Cancer Center Hospital, Chuo-ku, Tokyo; [5]Biomolecular Characterization Team, RIKEN, Wako, Saitama; [6]Laboratory for Medical Informatics, RIKEN, Yokohama, Kanagawa, Japan; Departments of [7]Genetics and [8]Oncology, Cancer Research UK, Cambridge Research Institute, University of Cambridge, Cambridge; [9]Institute of Ophthalmology, University College London, London, United Kingdom; and [10]Section of Hematology/Oncology, The University of Chicago, Chicago, Illinois

Note: Supplementary data for this article are available at Cancer Research Online (http://cancerres.aacrjournals.org/).

M. Takawa and H.-S. Cho contributed equally to this work.

Corresponding Author: Ryuji Hamamoto, Laboratory of Molecular Medicine, Human Genome Center, Institute of Medical Science, The University of Tokyo, 4-6-1 Shirokanedai, Minato-ku, Tokyo 108-8639, Japan. Phone: 81-3-5449-5233; Fax: 81-3-5449-5123; E-mail: ryuji@ims.u-tokyo.ac.jp

doi: 10.1158/0008-5472.CAN-11-3701

Published OnlineFirst May 3, 2012; DOI:10.1158/0008-5472.CAN-11-3701

to ubiquitination, it is estimated that approximately 6% of chromatin-bound PCNA is subjected to phosphorylation on Tyr 211 (11). It has been considered that phosphorylation of Tyr 211 on PCNA may stabilize chromatin-bound PCNA, as opposed to polyubiquitination. Furthermore, acetylation is another modification detected on PCNA (12), and in yeast, a poly-SUMOylation on PCNA has been described (13). However, functions of lysine methylation on PCNA have never been elucidated.

In this study, we showed that the histone methyltransferase SETD8 methylates Lys 248 on PCNA and regulates functions of PCNA in cancer cells. This is the first report to describe the significance of lysine methylation on PCNA.

Materials and Methods

Cell line

MRC-5, CCD-18Co, 5637, SW780, SCaBER, UMUC3, RT4, T24, HT-1376, A549, H2170, HCT116, LoVo, and 293T cells were from American Type Culture Collection in 2001 and 2003 and tested and authenticated by DNA profiling for polymorphic short tandem repeat (STR) markers, except for SW780. The SW780 line was established in 1974 by A. Leibovitz from a grade I transitional cell carcinoma. RERF-LC-AI and SBC5 cells were from Japanese Collection of Research Bioresources (JCRB) in 2001, and tested and authenticated by DNA profiling for polymorphic short tandem repeat (STR) markers. 253J and 253J-BV cells were from Korean Cell Line Bank (KCLB) in 2001, and tested and authenticated by DNA profiling for polymorphic STR markers. EJ28 cells were from Cell Line Service (CLS) in 2003, and tested and authenticated by DNA profiling for polymorphic STR markers. ACC-LC-319 cells were from Aichi Cancer Center in 2003, and tested and authenticated by DNA profiling for single-nucleotide polymorphism, mutation, and deletion analysis.

Tissue samples and RNA preparation

Bladder tissue samples and RNA preparation were described previously (14–17). Uroplakin is a marker of urothelial differentiation and is preserved in up to 90% of epithelially derived tumors (18). Use of tissues for this study was approved by Cambridgeshire Local Research Ethics Committee (Ref 03/018).

Quantitative real-time PCR

Specific primers for all human *GAPDH* (glyceraldehyde-3-phosphate dehydrogenase; housekeeping gene), *SDH* (housekeeping gene), *SETD8*, and *PCNA* were designed (primer sequences in Supplementary Table S1). PCR reactions were conducted with the LightCycler 480 System (Roche Applied Science) following the manufacturer's protocol.

siRNA transfection

siRNA oligonucleotide duplexes were purchased from Sigma-Genosys for targeting the human *SETD8* transcript. siEGFP, siFFLuc, and siNegative control (siNC), which is a mixture of 3 different oligonucleotide duplexes, were used as control siRNAs. The siRNA sequences are described in Supplementary Table S2. siRNA duplexes (100 nmol/L final concentration) were transfected into bladder and lung cancer cell lines with Lipofectamine 2000 (Life Technologies) for 72 hours, and cell viability was examined by Cell Counting Kit-8 (Dojindo).

Results

SETD8 is overexpressed in various types of cancer and regulates the growth of cancer cells

To investigate roles of a HKMT in human carcinogenesis, we had examined expression levels of several HKMTs in a small subset of clinical bladder cancer samples and found a significant difference in expression levels of *SETD8* between normal and cancer cells (data not shown). We then analyzed 124 bladder cancer samples and 28 normal control samples and confirmed the significant elevation of *SETD8* expression in tumor cells compared with normal cells (Supplementary Table S4). Expression levels partly correlated with the grade of malignancy in bladder cancer (Supplementary Fig. S1A). We also found overexpression of *SETD8* in both non–small cell lung carcinoma (NSCLC) and small cell lung carcinoma (SCLC; Fig. 1A). Subsequent immunohistochemical analysis using anti-SETD8 antibody identified strong SETD8 staining mainly in the nuclei of malignant cells, but no staining in nonneoplastic tissues (Fig. 1B). In addition, our expression profiling analysis indicated the upregulation of *SETD8* in chronic myelogenous leukemia, hepatocellular carcinoma, and pancreatic cancer (Supplementary Fig. S2 and Table S5). Furthermore, a high level of *SETD8* was identified in various cancer cell lines than in a normal lung cell line SAEC (Supplementary Fig. S3).

To investigate the role of SETD8 in the growth of cancer cells, we conducted a knockdown experiment using 2 independent siRNAs against SETD8 (siSETD8#1 and #2) and 2 control siRNAs (siEGFP and siFFLuc). We transfected each of these siRNAs into SW780 bladder cancer cells and found that SETD8 expression was efficiently suppressed by either of the 2 different siRNAs targeting SETD8, compared with control siRNAs (Supplementary Fig. S1B). Using the same siRNAs, we conducted cell growth assays and found significant growth-suppressive effects on 1 bladder cell line (SW780) and 2 lung cancer cell lines (RERF-LC-AI and SBC5), whereas no effect was observed when we used control siRNAs (Fig. 1C). Detailed cell-cycle analysis using flow cytometry indicated that the cell populations of cancer cells lacking SETD8 had a significant increase in the amount of S-phase and sub-G_1 phase cells and a concomitant reduction in the proportion of G_1 cells (Fig. 1D). Furthermore, we showed that in bromodeoxyuridine (BrdUrd) incorporation analysis, the amount of newly incorporated BrdUrd in cancer cells was significantly decreased after treatment with siSETD8 (Fig. 1E), implying that knockdown of SETD8 results in the retardation of DNA replication in cancer cells. These results indicated that SETD8 might play an important role in the regulation of cancer cell growth, especially in S-phase, and knockdown of SETD8 would cause apoptosis of cancer cells.

Published OnlineFirst May 3, 2012; DOI:10.1158/0008-5472.CAN-11-3701

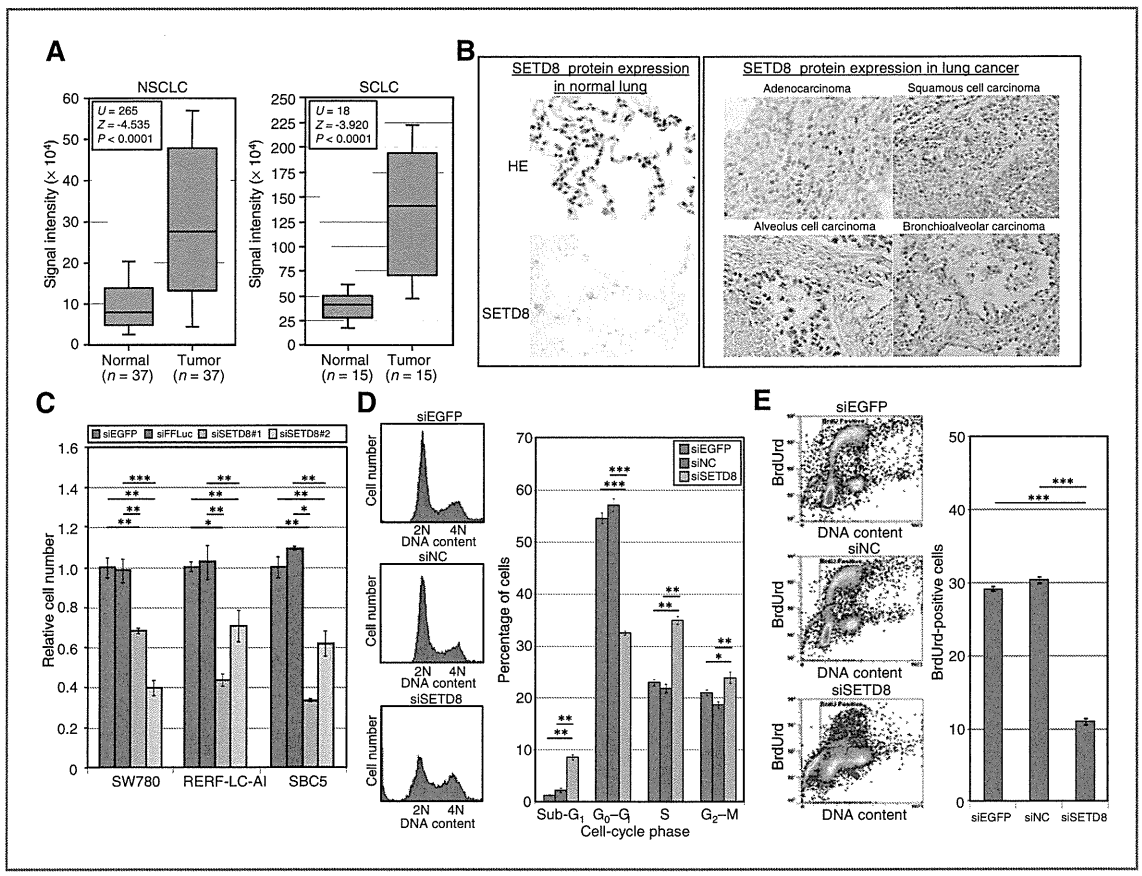

Figure 1. SETD8 is overexpressed in human cancer and regulates the proliferation of cancer cells. A, expression of *SETD8* is significantly increased in tumor tissues compared with normal Japanese patients. Signal intensity for each sample was analyzed by cDNA microarray. B, immunohistochemical staining of SETD8 in lung tissues. Clinical information for each section is represented above histologic pictures. Original magnification, × 100. HE, hematoxylin and eosin. C, effects of *SETD8* siRNA knockdown on the viability of bladder (SW780) and lung (RERF-LC-AI and SBC5) cancer cell lines. Relative cell numbers were normalized to the number of siEGFP-treated cells (siEGFP = 1): results are the mean ± SD of 3 independent experiments. *P* values were calculated using Student *t* test (*, $P < 0.05$; **, $P < 0.01$; ***, $P < 0.001$). D, effect of SETD8 knockdown on cell-cycle kinetics in cancer cells. Cell-cycle distribution was analyzed by flow cytometry after staining with propidium iodide (PI). Left, representative histograms of SBC5 cells stained with PI. Right, numerical analysis of fluorescence-activated cell-sorting (FACS) results in SBC5 cells, classifying cells by cell-cycle status. Results are the mean ± SD of 3 independent experiments. *P* values were calculated using Student *t* test (**, $P < 0.01$; ***, $P < 0.001$). E, detailed cell-cycle kinetics in SBC5 cells after treatment with siSETD8. Cell-cycle distribution was analyzed by flow cytometry after coupled staining with fluorescein isothiocyanate (FITC)-conjugated anti-BrdUrd and 7-amino-actinomycin D (7-AAD) as described in Materials and Methods.

SETD8 methylates lysine 248 of PCNA both *in vitro* and *in vivo*

As PCNA is known to be a key regulator of cell-cycle progression and SETD8 is a component of the PCNA complex (19, 20), we examined the functional relationship between SETD8 and PCNA. Immunoprecipitation assay showed that 3xFLAG-tagged SETD8 bound endogenous PCNA (Fig. 2A). We also confirmed the interaction between endogenous PCNA and SETD8 proteins (Fig. 2B); endogenous SETD8 and PCNA proteins were colocalized in HeLa cells (Fig. 2C). Immunoprecipitation using deletion mutants of SETD8 showed that its N-terminal region of SETD8 is essential for binding to PCNA (Fig. 2D), and this portion contains a PCNA-interacting protein (PIP) box (Supplementary Fig. S4A). Because histone methyltransferases have been found to methylate nonhistone substrates, we evaluated a possibility of PCNA to be a substrate of SETD8. First, we conducted an *in vitro* methyltransferase assay and confirmed that PCNA was methylated in a dose-dependent manner (Fig. 2E). The amino acid analysis detected a single lysine methylation site in PCNA following this reaction (Supplementary Fig. S5). To verify *in vivo* SETD8-dependent PCNA methylation, we labeled 293T cells after transfection with FLAG-PCNA (WT) and hemagglutinin (HA)-mock or HA-SETD8 (1-352) expression vectors with L-[methyl-^{3}H] methionine and found that SETD8 could methylate PCNA *in vivo* (Supplementary Fig. S6A). Subsequent liquid chromatography/tandem mass spectrometry (LC/MS-MS) analysis identified monomethylation at lysine 248 on PCNA by SETD8 (Fig. 2F). To

Published OnlineFirst May 3, 2012; DOI:10.1158/0008-5472.CAN-11-3701

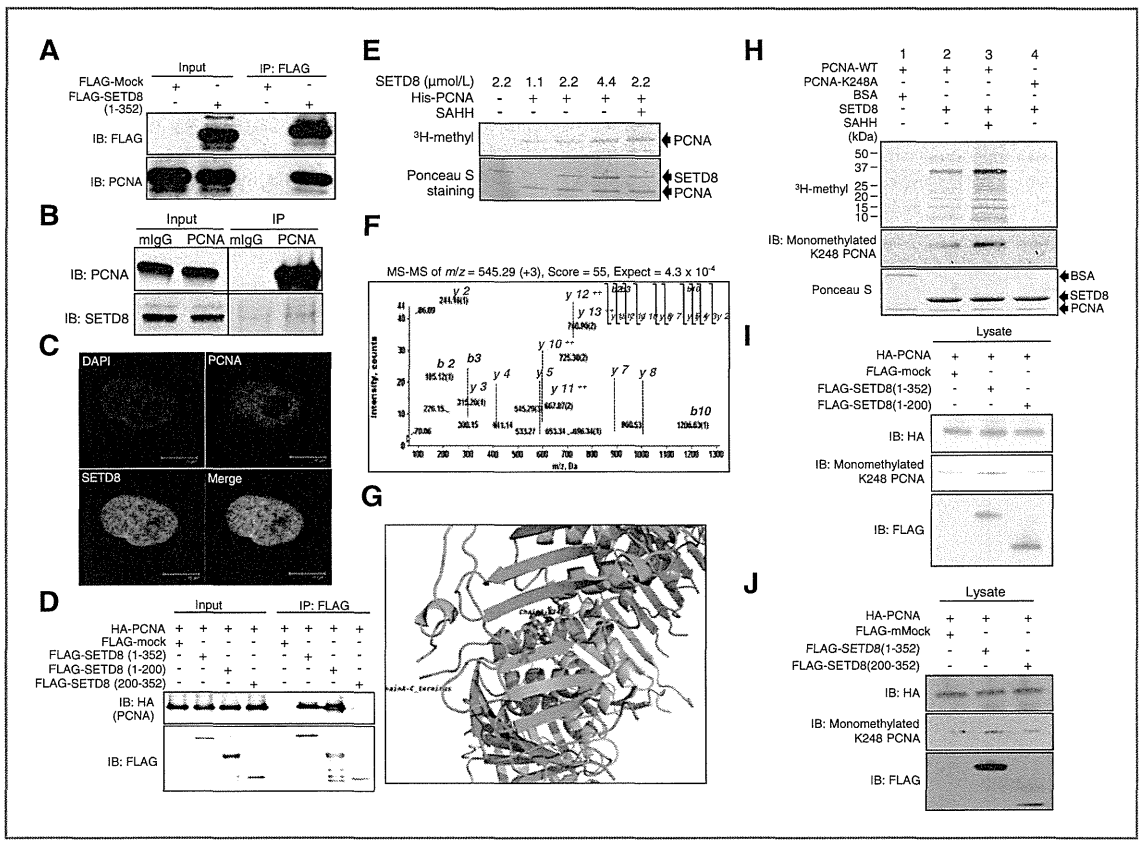

Figure 2. SETD8 methylates lysine 248 of PCNA both *in vitro* and *in vivo*. A, FLAG-mock and FLAG-SETD8 expression vectors were transfected into 293T cells. After 48 hours, cells were immunoprecipitated (IP) with anti-FLAG M2 agarose beads, and immunoprecipitants were immunoblotted (IB) with anti-FLAG (F7425; Sigma-Aldrich) and anti-PCNA (PC10, Santa Cruz Biotechnology) antibodies, respectively. B, SBC5 cells were lysed and immunoprecipitated with normal mouse IgG (mIgG) and anti-PCNA antibody (PC10). The immunoprecipitates were fractionated by SDS-PAGE and blotted with anti-PCNA (PC10) and anti-SETD8 (ab3798, Abcam) antibodies. C, immunocytochemical analysis of HeLa cells. Cells were stained with an anti-PCNA antibody [PC10, Cell Signaling Technology; Alexa Fluor 594 (red)], an anti-SETD8 antibody [C18B7, Cell Signaling Technology; Alexa Fluor 488 (green)], and 4′,6′-diamidine-2′-phenylindole dihydrochloride [DAPI (blue)]. D, 293T cells were transfected with HA-PCNA and FLAG-mock or indicated FLAG-SETD8 expression vectors containing deletion variants. Cell lysates were immunoprecipitated with anti-FLAG M2 agarose beads. Samples were fractionated by SDS-PAGE and blotted with anti-HA (Y-11, Santa Cruz Biotechnology) and anti-FLAG (F7425) antibodies. E, *in vitro* methyltransferase assay of PCNA. Recombinant His-PCNA and ^{3}H-SAM were incubated in the presence or absence of recombinant SETD8, and the reaction products were analyzed by SDS-PAGE followed by fluorography (top). The membrane was stained with Ponceau S (bottom). F, the MS-MS spectrum corresponding to the monomethylated PCNA 241–254 peptide. The 14 Da increase of the Lys 248 residue was observed, showing the monomethylated Lys 248. Score and Expect show Mascot Ion Score and Expectation value in Mascot Database search results, respectively. G, structure of the methylation site in PCNA protein analyzed by PyMOL. H, validation of an anti-monomethylated K248 PCNA antibody. Recombinant PCNA-WT or PCNA-K248A proteins and ^{3}H-SAM were incubated in the presence or absence of recombinant SETD8, and the reaction products were analyzed by SDS-PAGE followed by fluorography (top). The membrane was immunoblotted with an anti-monomethylated K248 antibody (middle) and stained with Ponceau S (bottom). BSA, bovine serum albumin. I and J, 293T cells were cotransfected with an HA-PCNA vector and an empty vector (FLAG-mock), a FLAG-SETD8 (1-352) vector, (1-200, ΔSET) vector, or a FLAG-SETD8 (200-352, ΔPIP box) vector. The samples were immunoblotted with anti-monomethylated K248 PCNA, anti-FLAG, and anti-HA antibodies. SAHH, *S*-adenosyl-L-homocysteine hydrolase.

validate this result, we constructed the plasmid (PCNA-K248A) that was designed to substitute lysine 248 of PCNA protein to alanine and conducted *in vitro* methyltransferase assay (Supplementary Fig. S6B). The intensity of the band corresponding to PCNA methylation in PCNA-K248A was significantly diminished compared with that of the wild-type PCNA (PCNA-WT). These data show that lysine 248, which is highly conserved in the PCNA ortholog from green alga to human (Supplementary Fig. S4B), is the primary target of SETD8-dependent methylation (Fig. 2G). On the basis of this result, we generated an antibody against a methylated K248 synthetic peptide (Supplementary Fig. S7A) that showed high affinity and high specificity by ELISA (Supplementary Fig. S7B). Western blot analysis using this antibody confirmed that it specifically recognizes K248-methylated PCNA (Fig. 2H and Supplementary Fig. S7C and S7D), and this specific signal was dependent on the methyltransferase activity of SETD8 (Fig. 2I). Importantly, the methyltransferase activity of N-terminal–deleted SETD8 protein, which lacks the PIP box domain, was significantly low than that of wild-type SETD8 protein (Fig. 2J). This

Published OnlineFirst May 3, 2012; DOI:10.1158/0008-5472.CAN-11-3701

result indicates that the N-terminal region of SETD8 containing PIP box domain seems to be important for SETD8-dependent PCNA methylation. This antibody was used to examine the methylation status of PCNA *in vivo* after treatment with siSETD8 (Supplementary Fig. S8). Monomethylation of PCNA at lysine 248 diminished after knockdown of SETD8 in SBC5 cells, implying SETD8-dependent PCNA K248 methylation occurs both *in vitro* and *in vivo*.

SETD8 stabilizes PCNA protein through the methylation of lysine 248

To clarify the physiologic significance of PCNA methylation by SETD8, we examined protein expression levels of PCNA in SW780 cells 48 hours after knockdown of SETD8 using 2 independent siRNAs (Fig. 3A). Knockdown of SETD8 decreased PCNA protein, suggesting involvement of SETD8 in regulating PCNA stability in cancer cells. To further validate this result, we examined the cell-cycle dependency of SETD8 and PCNA protein expression levels after aphidicolin synchronization (Fig. 3B). Intriguingly, when we treated with SETD8 siRNAs, PCNA protein expression decreased in both G_1 and S-phases according to the levels of SETD8, indicating that SETD8 is likely to be a key regulator of PCNA protein expression at G_1 and S-phases. Because quantitative real-time PCR analysis implied that *PCNA* mRNA level was not affected by treatment with siSETD8 (Fig. 3B), the regulation of PCNA expression by SETD8 was not at the transcriptional level but at the protein level. To examine that this regulation is mediated by SETD8-dependent methylation, we examined PCNA (WT) or PCNA (K248A) protein expression levels in 293T cells transfected with mock

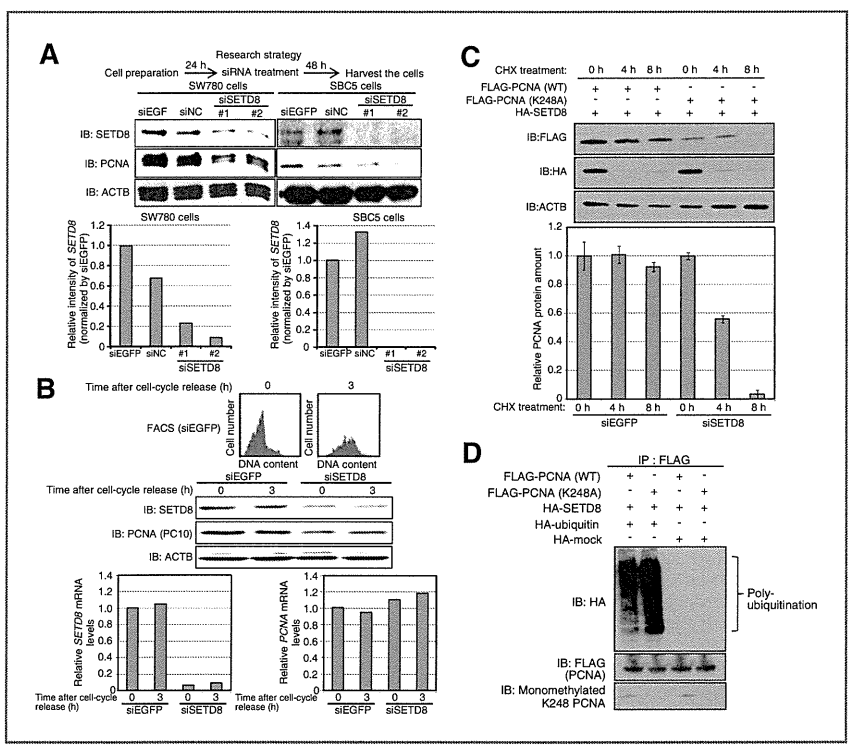

Figure 3. SETD8 stabilizes PCNA protein through the methylation of lysine 248. A, top, validation of SETD8 and PCNA expressions at the protein level. Lysates from SW780 and SBC5 cells, 48 hours after treatment with 2 control siRNAs (siEGFP and siNC) and 2 different siRNAs targeting SETD8 (siSETD8), were immunoblotted (IB) with anti-SETD8 (ab3798), anti-PCNA (PC10), and anti-ACTB (I-19, Santa Cruz Biotechnology) antibodies. β-actin (ACTB) served as an internal control. Bottom, the signal intensity corresponding SETD8 protein was quantified by ImageJ (http://rsb.info.nih.gov/ij/index.html). B, effects of SETD8 knockdown on the stability of PCNA in SW780 cells after synchronizing the cell cycle. SW780 cells were treated with siEGFP and siSETD8#2 for 24 hours and synchronized the cell cycle with 7.5 μg/mL aphidicolin. After 24 hours of treatment, the culture medium was changed, and the cells were collected at 0 and 3 hours after the release from cell-cycle arrest. Cell-cycle status was analyzed by FACS (top, red), and cell lysates were immunoblotted with anti-SETD8 (ab3798), anti-PCNA (PC10), and anti-ACTB (I-19) antibodies (middle). Expression of ACTB was the internal control. Transcriptional expression levels of *SETD8* and *PCNA* were quantified by real-time PCR (bottom). C, SETD8 stabilizes PCNA protein through K248 methylation. 293T cells were transfected with FLAG-PCNA (WT) or FLAG-PCNA (K248A) and HA-SETD8 (1-352) expression vectors. After 24 hours, cells were treated with 100 μg/mL of cycloheximide (CHX) for 4 and 8 hours, then immunoblotted with anti-HA (Y-11), anti-FLAG (F7425), and anti-ACTB (I-19) antibodies. Signal intensities of PCNA and ACTB proteins were quantitatively analyzed by GS-800 (Bio-Rad), and each PCNA intensity was normalized by ACTB intensity. Relative PCNA protein amount shows the intensity value standardized by the intensity at 0 hour (both siEGFP- and siSETD8-treated samples, 0 h = 1): results are the mean ± SD of triplicate experiments. D, ubiquitin assay of exogenous PCNA. FLAG-PCNA (WT) or FLAG-PCNA (K248A) and HA-SETD8 (1-352) expression vectors were transfected into 293T cells together with a HA-ubiquitin or HA-mock expression vector. Cell lysates were immunoprecipitated (IP) with anti-FLAG M2 agarose beads and immunoblotted with anti-FLAG (F7425), anti-HA (Y-11), and anti-monomethylated K248 PCNA antibodies.

Published OnlineFirst May 3, 2012; DOI:10.1158/0008-5472.CAN-11-3701

or SETD8 expression vectors after cycloheximide treatment. Although wild-type PCNA was significantly stabilized by SETD8 expression, methylation-inactive mutant PCNA (PCNA-K248A) was unstable (Fig. 3C). Furthermore, we examined the PCNA stability in endogenous level after depletion of SETD8 and found that the degradation rate of PCNA in cells treated with siSETD8 more rapidly than siEGFP (Supplementary Fig. S9). Taken together, SETD8-dependent methylation is crucial for PCNA stabilization. Then, we validated the effect of SETD8-dependent methylation on ubiquitination of PCNA proteins. The PCNA (WT) or PCNA (K248A) expression vector was cotransfected into 293T cells with a vector expressing either the full-length or N-terminal region of SETD8, and ubiquitination and methylation status of PCNA was examined (Fig. 3D). As we expected, the status of ubiquitination and methylation on PCNA showed the inverse correlation. Hence, we consider that methylation of PCNA inhibited its ubiquitination. We also examined the phosphorylation status of Tyr 211 on PCNA, which is known to influence the stability of PCNA (11), but no significant relationship between methylation and phosphorylation status was observed (data not shown). These data show that PCNA protein is stabilized through inhibition of the ubiquitination by its SETD8-dependent methylation.

Methylation of lysine 248 on PCNA affects its interaction with FEN1

We conducted immunoprecipitation analysis to further investigate the significance of PCNA methylation, using wild-type and methylation-inactive mutant PCNA proteins, and identified a partner protein, FEN1, which interacted with

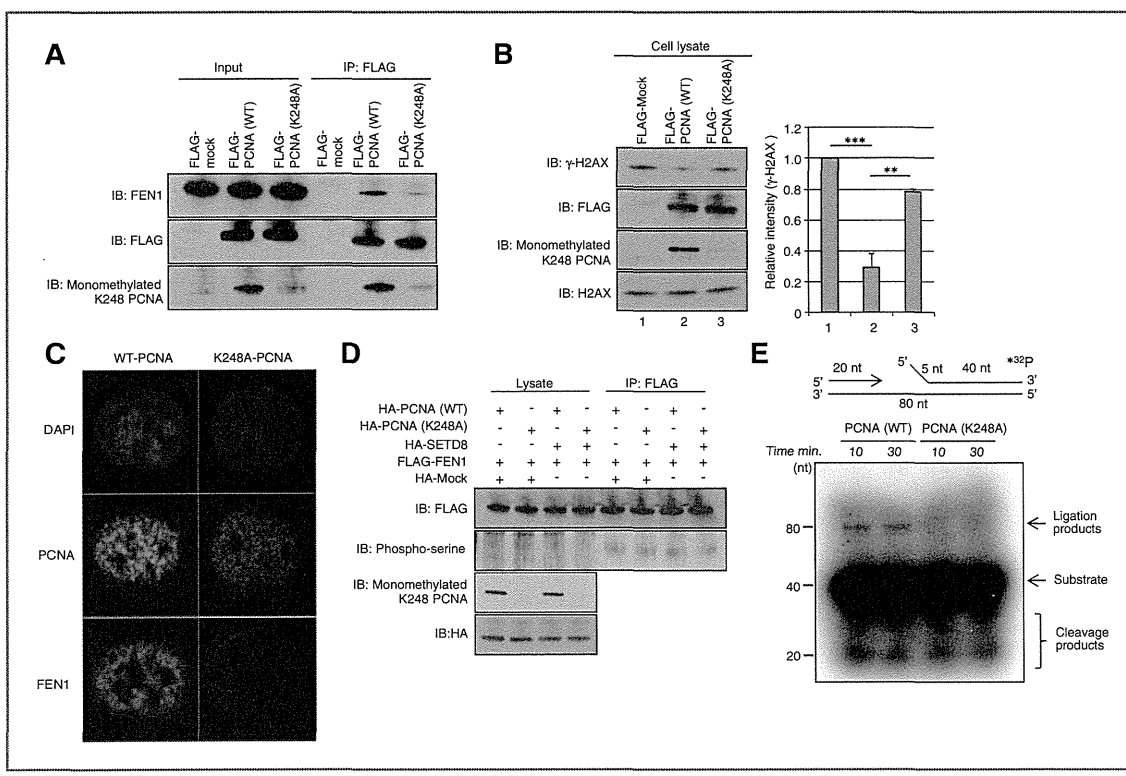

Figure 4. Methylation of PCNA is crucial for the interaction with FEN1. A, K248 monomethylation affected the interaction of PCNA with FEN1. 293T cells were transfected with a FLAG-PCNA (WT) vector or a FLAG-PCNA (K248A) vector together with an HA-SETD8 vector. Immunoprecipitation (IP) was conducted using anti-FLAG M2 agarose and samples were immunoblotted (IB) with anti-FLAG (F7425), anti-FEN1 (HPA006748, Sigma-Genosys), and anti-monomethylated K248 PCNA antibodies. B, double-strand DNA breaks were detected by Western blotting using an anti-γH2AX antibody (05-636, Millipore). Lysates from 293T cells transfected with a FLAG-PCNA (WT) or a FLAG-PCNA (K248A) and were immunoblotted with anti-FLAG (F7425), anti-monomethylated K248 PCNA, anti-γH2AX (05-636), and anti-H2AX (07-627, Millipore) antibodies. Signal intensity was quantified by ImageJ. Results are the mean of 2 independent experiments. C, subcellular localization of PCNA and FEN1 in S-phase. HeLa cells transfected with a FLAG-PCNA (WT) vector or a FLAG-PCNA (K248A) vector were synchronized at late G_1 phase by treatment with mimosine (400 μmol/L for 12 hours). Cell cycle was released by removing mimosine, and cells were costained with anti-FLAG (F7425) and anti-FEN1 (HPA006748) antibodies. Scale bar, 5 μm. D, methylation of PCNA does not alter FEN1 phosphorylation. 293T cells were cotransfected with a HA-PCNA (WT) vector or a HA-PCNA (K248A) together with HA-SETD8 and FLAG-FEN1 expression vectors. Immunoprecipitation was conducted using anti-FLAG M2 agarose, and samples were immunoblotted with anti-FLAG (F7425), anti-HA (Y-11), anti-monomethylated K248 PCNA, and anti-phospho-serine (4A4, Millipore) antibodies. E, Okazaki fragment maturation assay. A schematic diagram of the assay (top) showing a gap substrate (20 mer and 40 mer,top; with an 80-mer complementary strand, bottom) with a 5-nt DNA flap (40 mer, top right strand, with or without a ^{32}P label attached). The gap substrate was incubated with wild-type PCNA [FLAG-PCNA (WT)] and mutant-type PCNA [FLAG-PCNA (K248A)].

Published OnlineFirst May 3, 2012; DOI:10.1158/0008-5472.CAN-11-3701

PCNA in a methylation-dependent manner. Methylation of PCNA significantly enhanced the interaction between PCNA and FEN1 (Fig. 4A). To validate the effect of PCNA methylation on the interaction with FEN1 in more detail, we conducted an *in vitro* binding assay using methylated PCNA and unmethylated PCNA with FEN1 recombinant protein. SETD8-dependent lysine methylation of PCNA significantly enhanced the interaction between PCNA and FEN1 *in vitro* (Supplementary Fig. S10). FEN1 is a structure-specific nuclease with both 5′ flap endonuclease and 5′-3′ exonuclease activities (21). During DNA replication, this enzyme is responsible for RNA primer removal during Okazaki fragment processing and was identified as the factor responsible for the completion of replication *in vitro* (22). Yeast cells lacking the *FEN1* gene (also called *RAD27*) are viable but are unable to grow at high temperatures, indicating defective DNA replication (23). To examine the effect of PCNA methylation on FEN1 function, we measured levels of the phosphorylated form of H2AX histone variant (γH2AX), an early marker of the cellular response to DNA breaks. In the absence of any exogenous source of DNA damage, basal levels of phosphorylated γH2AX in 293T cells expressing methylation-inactive mutant PCNA (PCNA-K248A) were higher than those in 293T cells expressing wild-type PCNA (Fig. 4B). This implies the accumulation of DNA double-strand breaks resulting from methylation-inactive mutant PCNA expression. During the S-phase of the cell cycle, FEN1 is recruited to DNA replication loci through the interaction with PCNA. Disruption of the FEN1–PCNA interaction impairs such localization (24).

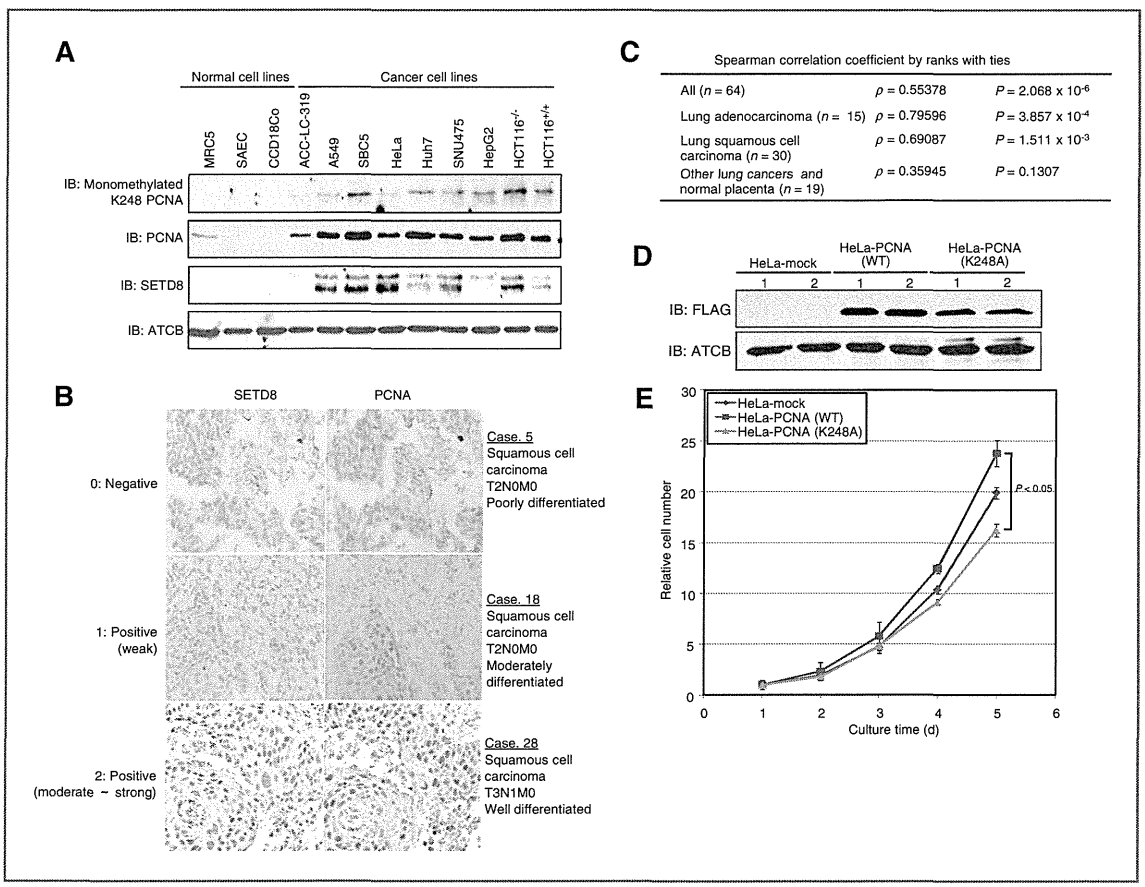

Figure 5. SETD8 and PCNA are coexpressed in lung cancer tissues, and methylation of PCNA promotes the proliferation of cancer cells. A, validation of PCNA methylation status in various cell lines. Lysates from normal cell lines and cancer cell lines were immunoblotted (IB) with anti-monomethylated K248 PCNA and anti-ACTB (I-19) antibodies. B, immunohistochemical stainings of SETD8 and PCNA in lung cancer tissues. Three typical stained case tissues are shown, with staining intensity of each case categorized into 3 patterns: 0 (no staining), 1 (weak staining), and 2 (moderate or strong staining). Detailed clinical information is described in Supplementary Table S6. C, correlation of staining between SETD8 and PCNA was statistically calculated using Spearman correlation coefficient by ranks with ties. D, construction of HeLa stable cell lines overexpressing wild-type PCNA [HeLa-PCNA (WT)] and K248-substituted PCNA [HeLa-PCNA (K248A)]. Empty vector–transfected HeLa stable cell lines were used as a control (HeLa-mock). Lysates from each cell line were immunoblotted with anti-FLAG (F7425) and anti-ACTB (I-19) antibodies. E, the cell growth assay was conducted using HeLa stable cell lines. Number of cells was measured by Cell Counting Kit-8 (Dojindo) and relative cell number shows the value normalized by the number of cells at day 1 (day 1 = 1). Results are the mean ± SD in 3 independent experiments. *P* values were calculated using Student *t* test.

Published OnlineFirst May 3, 2012; DOI:10.1158/0008-5472.CAN-11-3701

If methylation of PCNA were important for interacting with FEN1, failure in methylation would lead to a defect in FEN1's localization to replication foci. FEN1 could be colocalized with PCNA at replication foci in cells when PCNA was a wild-type. However, FEN1 was unable to localize to the foci in cells in which methylation-inactive mutant was present (Fig. 4C). These data suggest that PCNA methylation is important for regulation of FEN1's subnuclear localization. Because phosphorylation of FEN1 has been shown to abolish its PCNA interaction (25), we examined FEN1 phosphorylation status in cells expressing wild-type and methylation-inactive mutant PCNA, but found no significant difference in phosphorylation status of FEN1 between wild-type and methylation-inactive mutant PCNA–expressing cells (Fig. 4D). This implies that the different affinity between PCNA and FEN1 seems to be regulated not by phosphorylation status of FEN1 but by methylation status of PCNA (as shown in Fig. 4A and C). Furthermore, an Okazaki fragment maturation assay was conducted using the deoxynucleotide triphosphate mixture containing radiolabeled dCTP and a model substrate containing an RNA-DNA flap, which mimicked the Okazaki fragment maturation intermediate. The assay simulates the sequential reactions of gap filling, RNA primer removal, and DNA ligation during Okazaki fragment maturation. When the assay was conducted *in vitro*, nuclear extracts from PCNA-K248A–expressing cells showed significant decrease in removing RNA primer flaps and some extent of defect in DNA ligation (Fig. 4E), indicating that the methylation defect of PCNA retarded Okazaki fragment maturation. Defects in the Okazaki fragment maturation process during DNA replication or defects in ligation during DNA repair could lead to accumulation of DNA double-strand breaks (26, 27). To examine the levels of double-strand breaks, 293 cells expressing wild-type and methylation-inactive mutant PCNA were treated with H_2O_2 to determine the survival rate (Supplementary Fig. S11). Consistent with previous data, methylation-inactive mutant PCNA–expressing cells were more sensitive to H_2O_2.

SETD8 and PCNA are coexpressed in lung cancer tissues, and lysine 248 methylation of PCNA promotes the proliferation of cancer cells

We then compared the methylation of endogenous PCNA in normal and cancer cell lines. PCNA was significantly methylated in various types of cancer cell lines, whereas no detectable level of PCNA methylation was found in normal cell lines (Fig. 5A). We subsequently conducted the immunopathologic analysis on clinical lung tissues, analyzing the correlation between SETD8 and PCNA protein expression levels (Fig. 5B). Clinical information and staining patterns of clinical tissues are described in Table 1 and Supplementary Table S6. We found

Table 1. Association between SETD8 and PCNA in lung cancer tissues and patients' characteristics (N = 64)

	Number of cases	SETD8 expression positive	SETD8 expression negative	PCNA expression positive	PCNA expression negative
	n = 64	*n* = 42	*n* = 22	*n* = 48	*n* = 16
Gender	62	40	22	46	16
Male	40	25	15	32	8
Female	22	15	7	14	8
Age, y	62	40	22	46	16
<65	42	28	14	32	10
≥65	20	12	8	14	6
Histologic type	64	42	22	48	16
ADC	14	10	4	10	4
SCC	30	17	13	20	10
Others[a]	20	15	5	18	2
pT factor	63	42	21	48	15
pT0	4	3	1	3	1
pT1	7	7	0	7	0
pT2	41	25	16	29	12
pT3	11	7	4	9	2
pN factor	59	40	19	44	15
N0	48	33	15	34	14
N1	11	7	4	10	1
M factor	61	41	20	46	15
M0	59	40	19	44	15
M1	2	1	1	2	0

Abbreviations: ADC, adenocarcinoma; ASC, adenosquamous-cell carcinoma; LCC, large cell carcinoma; SCC, squamous cell carcinoma.

[a]Others include SCLC, LCC, and ASC.

Published OnlineFirst May 3, 2012; DOI:10.1158/0008-5472.CAN-11-3701

a correlation factor (ρ) of 0.55378 with P value of 2.068×10^{-6} (by Spearman correlation coefficient) in a cohort of 64 cases (Fig. 5C); lung adenocarcinoma showed a stronger correlation ($\rho = 0.79596$, $P = 3.857 \times 10^{-4}$), supporting our hypothesis that SETD8 overexpression stabilizes and increases the PCNA protein expression in cancer cells. Finally, we examined the effect of PCNA methylation on the growth of cancer cells (Fig. 5D and E). Methylation-inactive–type PCNA–expressing HeLa cells (HeLa-PCNA-K248A) showed a slower growth rate than those with wild-type PCNA–expressing HeLa cells (HeLa-PCNA-WT). Furthermore, to exclude the effect of endogenous PCNA proteins, we first knocked down *PCNA* gene expression, and then, conducted a clonogenecity assay of HeLa cells overexpressing wild-type PCNA and methylation-inactive-type PCNA (Supplementary Fig. S12). Consistent with our previous data, wild-type PCNA showed higher growth promoting effects than methylation-inactive type PCNA. Taken together, these results imply that methylation of PCNA is likely to play a crucial role in the growth promotion of cancer cells.

Discussion

Histone lysine methylation plays a central epigenetic role in the organization of chromatin domains and the regulation of gene expression. We previously reported that the HKMT SMYD3 stimulates cell proliferation through its methyltransferase activity and plays a crucial role in human carcinogenesis (28, 29). Of the various posttranslational protein modifications, the role of protein methylation in signal transduction has not been well characterized. While the carboxyl group and arginine methylation have been implicated in several cellular responses, including receptor signaling, protein transport, and transcription (30), lysine methylation has been considered to be histone specific (31). In the present study, we found that the HKMT SETD8 is overexpressed in various types of cancer and regulates PCNA functions through the methylation of lysine 248. This is a new mechanism revealing the importance of lysine methylation in nonhistone proteins in human cancer.

PCNA was originally reported to be a DNA-sliding clamp for replicative DNA polymerases and is an essential component of the eukaryotic chromosomal DNA replisome (32, 33). It interacts with multiple partners including proteins involved in Okazaki fragment processing, DNA repair, DNA synthesis, DNA methylation, chromatin remodeling, and cell-cycle regulation (34). PCNA has been reported to be modified by ubiquitination, SUMOylation, phosphorylation, and acetylation (9, 11, 12, 35, 36) but its lysine methylation has never been. These kinds of protein modifications are vital for a wide variety of PCNA functions. As reported here, PCNA protein is stably overexpressed in various types of cancer cells, together with SETD8 protein, indicating that SETD8-dependent methylation of PCNA enhances its biologic activity. Knockdown of SETD8 significantly suppressed the growth of cancer cells by diminishing PCNA methylation and reduction of its protein levels. It has been recently reported that knockdown of SETD8 leads to several aberrant phenotypes, including DNA damage, S-phase arrest, and global chromosome condensation (20, 37, 38), consistent with our findings, which suggest that these abnormalities is likely to be caused by dysfunction of the PCNA protein.

PCNA is also considered to be the crucial factor in maintaining the balance between survival and cell death. For instance, PCNA displays an apoptotic activity through interaction with proteins belonging to the Gadd45 family (Gadd45, Myd118, and CR6), which was involved in growth control, apoptosis, and DNA repair (39, 40). Lack of SETD8 induces an increase of the sub-G_1 population of cancer cells (Fig. 1D), so it is possible that apoptosis may be induced by SETD8 depletion through dysfunction of PCNA. Furthermore, we clarified that methylation of PCNA is critical for the interaction with FEN1. It has been reported that FEN1 forms distinct protein complexes for DNA replication and repair. Through its interaction with PCNA, FEN1 is recruited to the replication foci for RNA primer removal and to repair sites for DNA base excision repair (41). Recently, the FEN1–PCNA interaction has been implicated in coordinating the sequential action of polymerase δ (Pol δ), FEN1, and DNA ligase 1 (Lig1) during Okazaki fragment maturation (24). Disruption of PCNA–FEN1 interaction impairs Okazaki fragment ligation (24). We showed that methylation-defective PCNA retards both Okazaki fragment maturation and DNA replication, and induces DNA damages. Cells expressing methylation-inactive mutant PCNA were more sensitive to DNA damage. Because deregulation of FEN1 nuclease has also been reported to be linked to human cancer (42), it is possible that abnormal interactions between FEN1 and PCNA may cause human carcionogenesis. Intriguingly, Guo and colleagues recently showed that methylation of FEN1 suppresses nearby phosphorylation and facilitates PCNA binding (43). Together with our result, this implicates methylation as the crucial player in the interaction between PCNA and FEN1 proteins.

In conclusion, as expression levels of *SETD8* in normal tissues are significantly low (Supplementary Fig. S13), an inhibitor targeting its enzymatic activity might be an effective drug for cancer therapy. Further functional analysis will explore the SETD8-dependent PCNA methylation pathway as a therapeutic target in various types of cancer.

Disclosure of Potential Conflicts of Interest

Y. Yamane, Y. Iwai, and K. Maejima are employed as Researchers in OncoTherapy Science, Inc. R. Hamamoto is a scientific advisor in OncoTherapy Science, Inc. The other authors disclosed no potential conflicts of interest.

Authors' Contributions

Conception and design: M. Takawa, H.-S. Cho, S. Hayami, G. Toyokawa, M. Sugiyama, Y. Nakamura, R. Hamamoto

Development of methodology: M. Takawa, H.-S. Cho, S. Hayami, K. Ueda, N. Dohmae, R. Hamamoto

Acquisition of data (provided animals, acquired and managed patients, provided facilities, etc.): M. Takawa, M. Kogure, K. Ueda, A. Masuda, N. Dohmae, B.A.J. Ponder, R. Hamamoto

Analysis and interpretation of data (e.g., statistical analysis, biostatistics, computational analysis): M. Takawa, H.-S. Cho, M. Kogure, Y. Yamane, Y. Iwai, K. Maejima, K. Ueda, A. Masuda, N. Dohmae, T. Tsunoda, T. Akasu, M. Sugiyama, R. Hamamoto

Writing, review, and/or revision of the manuscript: M. Takawa, H.-S. Cho, K. Ueda, H.I. Field, T. Akasu, S. Ohnuma, Y. Nakamura, R. Hamamoto

Published OnlineFirst May 3, 2012; DOI:10.1158/0008-5472.CAN-11-3701

Administrative, technical, or material support (i.e., reporting or organizing data, constructing databases): M. Takawa, H.-S. Cho, Y. Yamane, Y. Iwai, K. Maejima, M. Sugiyama, R. Hamamoto
Study supervision: M. Takawa, M. Sugiyama, Y. Atomi, S. Ohnuma, B.A.J. Ponder, R. Hamamoto

Acknowledgments

The authors thank Kazuyuki Hayashi, Noriko Ikawa, and Haruka Sawada for technical assistance.

Grant Support

This work was supported by Grant-in Aid for Young Scientists (A; 22681030) from the Japan Society for the Promotion of Science.

The costs of publication of this article were defrayed in part by the payment of page charges. This article must therefore be hereby marked *advertisement* in accordance with 18 U.S.C. Section 1734 solely to indicate this fact.

Received November 8, 2011; revised April 24, 2012; accepted April 25, 2012; published OnlineFirst May 3, 2012.

References

1. Jenuwein T, Allis CD. Translating the histone code. Science 2001;293:1074–80.
2. Volkel P, Angrand PO. The control of histone lysine methylation in epigenetic regulation. Biochimie 2007;89:1–20.
3. Stoimenov I, Helleday T. PCNA on the crossroad of cancer. Biochem Soc Trans 2009;37:605–13.
4. Miyachi K, Fritzler MJ, Tan EM. Autoantibody to a nuclear antigen in proliferating cells. J Immunol 1978;121:2228–34.
5. Bravo R, Fey SJ, Bellatin J, Larsen PM, Celis JE. Identification of a nuclear polypeptide ("cyclin") whose relative proportion is sensitive to changes in the rate of cell proliferation and to transformation. Prog Clin Biol Res 1982;85:235–48.
6. Celis JE, Bravo R, Larsen PM, Fey SJ. Cyclin: a nuclear protein whose level correlates directly with the proliferative state of normal as well as transformed cells. Leuk Res 1984;8:143–57.
7. Prelich G, Tan CK, Kostura M, Mathews MB, So AG, Downey KM, et al. Functional identity of proliferating cell nuclear antigen and a DNA polymerase-delta auxiliary protein. Nature 1987;326:517–20.
8. Tan CK, Castillo C, So AG, Downey KM. An auxiliary protein for DNA polymerase-delta from fetal calf thymus. J Biol Chem 1986;261:12310–6.
9. Hoege C, Pfander B, Moldovan GL, Pyrowolakis G, Jentsch S. RAD6-dependent DNA repair is linked to modification of PCNA by ubiquitin and SUMO. Nature 2002;419:135–41.
10. Bailly V, Lauder S, Prakash S, Prakash L. Yeast DNA repair proteins Rad6 and Rad18 form a heterodimer that has ubiquitin conjugating, DNA binding, and ATP hydrolytic activities. J Biol Chem 1997;272:23360–5.
11. Wang SC, Nakajima Y, Yu YL, Xia W, Chen CT, Yang CC, et al. Tyrosine phosphorylation controls PCNA function through protein stability. Nat Cell Biol 2006;8:1359–68.
12. Naryzhny SN, Lee H. The post-translational modifications of proliferating cell nuclear antigen: acetylation, not phosphorylation, plays an important role in the regulation of its function. J Biol Chem 2004;279:20194–9.
13. Windecker H, Ulrich HD. Architecture and assembly of poly-SUMO chains on PCNA in *Saccharomyces cerevisiae*. J Mol Biol 2008;376:221–31.
14. Hayami S, Kelly JD, Cho HS, Yoshimatsu M, Unoki M, Tsunoda T, et al. Overexpression of LSD1 contributes to human carcinogenesis through chromatin regulation in various cancers. Int J Cancer 2011;128:574–86.
15. Hayami S, Yoshimatsu M, Veerakumarasivam A, Unoki M, Iwai Y, Tsunoda T, et al. Overexpression of the JmjC histone demethylase KDM5B in human carcinogenesis: involvement in the proliferation of cancer cells through the E2F/RB pathway. Mol Cancer 2010;9:59.
16. Wallard MJ, Pennington CJ, Veerakumarasivam A, Burtt G, Mills IG, Warren A, et al. Comprehensive profiling and localisation of the matrix metalloproteinases in urothelial carcinoma. Br J Cancer 2006;94:569–77.
17. Yoshimatsu M, Toyokawa G, Hayami S, Unoki M, Tsunoda T, Field HI, et al. Dysregulation of PRMT1 and PRMT6, type I arginine methyltransferases, is involved in various types of human cancers. Int J Cancer 2011;128:562–73.
18. Olsburgh J, Harnden P, Weeks R, Smith B, Joyce A, Hall G, et al. Uroplakin gene expression in normal human tissues and locally advanced bladder cancer. J Pathol 2003;199:41–9.
19. Huen MS, Sy SM, van Deursen JM, Chen J. Direct interaction between SET8 and proliferating cell nuclear antigen couples H4-K20 methylation with DNA replication. J Biol Chem 2008;283:11073–7.
20. Jorgensen S, Elvers I, Trelle MB, Menzel T, Eskildsen M, Jensen ON, et al. The histone methyltransferase SET8 is required for S-phase progression. J Cell Biol 2007;179:1337–45.
21. Lieber MR. The FEN-1 family of structure-specific nucleases in eukaryotic DNA replication, recombination and repair. Bioessays 1997;19:233–40.
22. Waga S, Bauer G, Stillman B. Reconstitution of complete SV40 DNA replication with purified replication factors. J Biol Chem 1994;269:10923–34.
23. Reagan MS, Pittenger C, Siede W, Friedberg EC. Characterization of a mutant strain of *Saccharomyces cerevisiae* with a deletion of the RAD27 gene, a structural homolog of the RAD2 nucleotide excision repair gene. J Bacteriol 1995;177:364–71.
24. Zheng L, Dai H, Qiu J, Huang Q, Shen B. Disruption of the FEN-1/PCNA interaction results in DNA replication defects, pulmonary hypoplasia, pancytopenia, and newborn lethality in mice. Mol Cell Biol 2007;27:3176–86.
25. Henneke G, Koundrioukoff S, Hubscher U. Phosphorylation of human Fen1 by cyclin-dependent kinase modulates its role in replication fork regulation. Oncogene 2003;22:4301–13.
26. Soza S, Leva V, Vago R, Ferrari G, Mazzini G, Biamonti G, et al. DNA ligase I deficiency leads to replication-dependent DNA damage and impacts cell morphology without blocking cell cycle progression. Mol Cell Biol 2009;29:2032–41.
27. Tishkoff DX, Filosi N, Gaida GM, Kolodner RD. A novel mutation avoidance mechanism dependent on *S. cerevisiae* RAD27 is distinct from DNA mismatch repair. Cell 1997;88:253–63.
28. Hamamoto R, Furukawa Y, Morita M, Iimura Y, Silva FP, Li M, et al. SMYD3 encodes a histone methyltransferase involved in the proliferation of cancer cells. Nat Cell Biol 2004;6:731–40.
29. Hamamoto R, Silva FP, Tsuge M, Nishidate T, Katagiri T, Nakamura Y, et al. Enhanced SMYD3 expression is essential for the growth of breast cancer cells. Cancer Sci 2006;97:113–8.
30. McBride AE, Silver PA. State of the arg: protein methylation at arginine comes of age. Cell 2001;106:5–8.
31. Lachner M, Jenuwein T. The many faces of histone lysine methylation. Curr Opin Cell Biol 2002;14:286–98.
32. Kelman Z, O'Donnell M. Structural and functional similarities of prokaryotic and eukaryotic DNA polymerase sliding clamps. Nucleic Acids Res 1995;23:3613–20.
33. Wyman C, Botchan M. DNA replication. A familiar ring to DNA polymerase processivity. Curr Biol 1995;5:334–7.
34. Moldovan GL, Pfander B, Jentsch S. PCNA, the maestro of the replication fork. Cell 2007;129:665–79.
35. Arakawa H, Moldovan GL, Saribasak H, Saribasak NN, Jentsch S, Buerstedde JM. A role for PCNA ubiquitination in immunoglobulin hypermutation. PLoS Biol 2006;4:e366.
36. Leach CA, Michael WM. Ubiquitin/SUMO modification of PCNA promotes replication fork progression in *Xenopus laevis* egg extracts. J Cell Biol 2005;171:947–54.
37. Houston SI, McManus KJ, Adams MM, Sims JK, Carpenter PB, Hendzel MJ, et al. Catalytic function of the PR-Set7 histone H4 lysine 20 monomethyltransferase is essential for mitotic entry and genomic stability. J Biol Chem 2008;283:19478–88.

Published OnlineFirst May 3, 2012; DOI:10.1158/0008-5472.CAN-11-3701

38. Tardat M, Murr R, Herceg Z, Sardet C, Julien E. PR-Set7-dependent lysine methylation ensures genome replication and stability through S-phase. J Cell Biol 2007;179:1413–26.
39. Azam N, Vairapandi M, Zhang W, Hoffman B, Liebermann DA. Interaction of CR6 (GADD45gamma) with proliferating cell nuclear antigen impedes negative growth control. J Biol Chem 2001;276:2766–74.
40. Vairapandi M, Balliet AG, Fornace AJ Jr, Hoffman B, Liebermann DA. The differentiation primary response gene MyD118, related to GADD45, encodes for a nuclear protein which interacts with PCNA and p21WAF1/CIP1. Oncogene 1996;12:2579–94.
41. Chen U, Chen S, Saha P, Dutta A. p21Cip1/Waf1 disrupts the recruitment of human Fen1 by proliferating-cell nuclear antigen into the DNA replication complex. Proc Natl Acad Sci U S A 1996;93:11597–602.
42. Zheng L, Jia J, Finger LD, Guo Z, Zer C, Shen B. Functional regulation of FEN1 nuclease and its link to cancer. Nucleic Acids Res 2011;39:781–94.
43. Guo Z, Zheng L, Xu H, Dai H, Zhou M, Pascua MR, et al. Methylation of FEN1 suppresses nearby phosphorylation and facilitates PCNA binding. Nat Chem Biol 2010;6:766–73.

Identification of a novel oncogene, *MMS22L*, involved in lung and esophageal carcinogenesis

MINH-HUE NGUYEN[1], KOJI UEDA[1,4], YUSUKE NAKAMURA[1] and YATARO DAIGO[1-3]

[1]Laboratory of Molecular Medicine, Human Genome Center, Institute of Medical Science, The University of Tokyo, Tokyo; [2]Department of Medical Oncology and [3]Cancer Center, Shiga University of Medical Science, Otsu; [4]Laboratory for Biomarker Development, Center for Genomic Medicine, RIKEN Yokohama Institute, Yokohama, Japan

Received April 27, 2012; Accepted June 12, 2012

DOI: 10.3892/ijo.2012.1589

Abstract. Genome-wide gene expression profile analyses using a cDNA microarray containing 27,648 genes or expressed sequence tags identified *MMS22L* (methyl methanesulfonate-sensitivity protein 22-like) to be overexpressed in the majority of clinical lung and esophageal cancers, but not expressed in normal organs except testis. Transfection of siRNAs against *MMS22L* into cancer cells suppressed its expression and inhibited cell growth, while exogenous expression of MMS22L enhanced the growth of mammalian cells. MMS22L protein was translocated to the nucleus and stabilized by binding to C-terminal portion of NFKBIL2 [nuclear factor of kappa (NFKB) light polypeptide gene enhancer in B-cells inhibitor-like 2]. Expression of a C-terminal portion of NFKBIL2 protein including the MMS22L-interacting site in cancer cells could reduce the levels of MMS22L in nucleus and suppressed cancer cell growth. Interestingly, reduction of MMS22L by siRNAs in cancer cells inhibited the TNF-α-dependent activation of RelA/p65 in the NFKB pathway and expression of its downstream anti-apoptotic molecules such as Bcl-XL and TRAF1. In addition, knockdown of MMS22L expression also enhanced the apoptosis of cancer cells that were exposed to DNA-damaging agents including 5-FU and CDDP. Our data strongly suggest that targeting MMS22L as well as its interaction with NFKBIL2 could be a promising strategy for novel cancer treatments, and also improve the efficacy of DNA damaging anticancer drugs.

Introduction

Lung cancer is the most common cause of cancer-related death, and the worldwide annual death by lung cancer was estimated to be 1.3 million (1). Esophageal squamous cell carcinoma (ESCC) is one of the most common gastrointestinal tract cancers in Asian countries (2). Although a huge body of knowledge about the biology of lung or esophageal carcinogenesis has been accumulated, the development of novel cancer therapeutics remains inefficient to improve patients with these cancers (3). In fact, in spite of development of various molecular targeted therapies, a limited proportion of patients can receive clinical benefit from them (4).

Through genome-wide gene expression analysis of lung and esophageal cancers, we have isolated a number of oncogenes that were involved in the development and/or progression of cancer (5-41). Among the genes upregulated in these cancers, we focused on *MMS22L* (methyl methanesulfonate-sensitivity protein 22-like) which is highly expressed in the majority of clinical lung and esophageal cancers. Our original gene expression profile database also revealed that this gene is highly expressed in clinical cervical cancers, but scarcely expressed in normal tissues except testis, suggesting that *MMS22L* encodes a cancer-testis antigen that can be defined by predominant expression in various types of cancer and undetectable expression in normal tissues except germ cells in testis or ovary (4). Cancer-testis antigens are considered to be good candidate molecular targets for developing new therapeutic strategies for cancers.

Constitutive activation of the NFKB pathway is involved in some forms of cancer such as leukemia, lymphoma, colon cancer and ovarian cancer as well as inflammatory diseases (42-45). The main mechanism of this pathway is reported to be the inactivation of IκB proteins by mutations as well as amplifications and rearrangements of genes encoding the NFKB transcription factor subunits (42-45). However, more commonly it is thought that changes in the upstream pathways that lead to NFKB activation are likely to be aberrantly upregulated in cancer cells (45). Recently some reports suggested that MMS22L-NFKBIL2 interaction could be essential for genomic stability and homologous recombination in immortalized cell lines, suggesting MMS22L to be a new regulator of DNA replication in human cells (46-49). However, no study has indicated critical roles of activation of MMS22L and NFKBIL2 in clinical cancers and investigated their functional importance in carcinogenesis. Here, we report that MMS22L is involved

Correspondence to: Professor Yataro Daigo, Department of Medical Oncology, Shiga University of Medical Science, Seta Tsukinowa-cho, Shiga 520-2192, Otsu, Japan
E-mail: ydaigo@ims.u-tokyo.ac.jp

Key words: MMS22L, oncogenes, therapeutic target, lung cancer, esophageal cancer

in NFKB pathway in cancer cells through its interaction with NFKBIL2 and might be a promising target for development of novel cancer therapy.

Materials and methods

Cell lines and clinical samples. The 12 human lung-cancer cell lines used for in this study included nine NSCLC cell lines (A549, NCI-H1373, LC319, NCI-H1781, PC-14, NCI-H358, NCI-H2170, NCI-H520 and LU61) and three small-cell lung cancer (SCLC) cell lines (SBC-3, SBC-5 and DMS114). The 9 human esophageal carcinoma cell lines used in this study were as follows: eight SCC cell lines (TE1, TE3, TE8, TE9, TE10, TE12, TE13 and TE15) and one adenocarcinoma (ADC) cell line (TE7). A cervical cancer cell line HeLa was also included in the study. All cells were grown in monolayers in appropriate media supplemented with 10% fetal calf serum (FCS) and were maintained at 37°C in an atmosphere of humidified air with 5% CO_2. Human airway epithelial cells, SAEC (Cambrex Bio Science Inc.), were also included in the panel of the cells used in this study. Primary lung and esophageal cancer samples had been obtained earlier with informed consent (5-10). This study and the use of all clinical materials mentioned were approved by individual institutional ethics committees.

Semiquantitative RT-PCR. We prepared appropriate dilutions of each single-stranded cDNA prepared from mRNAs of clinical lung and esophageal cancer samples, taking the level of β-actin (*ACTB*) expression as a quantitative control. The primer sets for amplification were as follows: *ACTB*-F (5'-GAGGTGATAGCA TTGCTTTCG-3') and *ACTB*-R (5'-CAAGTCAGTGTACAGG TAAGC-3') for *ACTB*, *MMS22L*-F (5'-GTCTCACCTTGGAC AGATGG-3') and *MMS22L*-R (5'-CCAAGGATCCTATTACA CAGTTGC-3') for *MMS22L*. All reactions involved initial denaturation at 95°C for 5 min followed by 22 (for *ACTB*) or 30 (for *MMS22L*) cycles of 95°C for 30 sec, 56°C for 30 sec, and 72°C for 60 sec on a GeneAmp PCR system 9700 (Applied Biosystems).

Northern blot analysis. Human multiple-tissue northern blots (16 normal tissues including heart, brain, placenta, lung, liver, skeletal muscle, kidney, pancreas, spleen, thymus, prostate, testis, ovary, small intestine, colon, leukocyte; BD Biosciences Clontech) were hybridized with a ^{32}P-labeled PCR product of *MMS22L*. The partial-length cDNA of *MMS22L* was prepared by RT-PCR using primers *MMS22L*-F1 (CTGGAAGAGGCA GTTGAAAA) and *MMS22L*-R1 (ATCGCCCAATATACTG CTCA). Prehybridization, hybridization, and washing were performed according to the supplier's recommendations. The blots were autoradiographed with intensifying screens at -80°C for 7 days.

Anti-MMS22L antibody. Synthesized peptide with the amino acids sequence of CLGQMGQDEMQRLENDNT [1227-1243] (Cysteine was added to the N-terminal) was inoculated into rabbits; the immune sera were purified on affinity columns according to standard methodology. Affinity-purified anti-MMS22L antibodies were used for western blot as well as immunocytochemical analyses. We confirmed that the antibody was specific to MMS22L on western blots using lysates from cell lines that had been transfected with MMS22L expression vector as well as those from lung and esophageal cancer cell lines that endogenously expressed MMS22L or not.

Western blot analysis. Cells were lysed in lysis buffer; 50 mM Tris-HCl (pH 8.0), 150 mM NaCl, 0.5% NP-40, 0.5% deoxycholate-Na, 0.1% SDS, plus protease inhibitor (Protease Inhibitor Cocktail Set III; Calbiochem). We used ECL western blot analysis system (GE Healthcare Bio-Sciences), as described previously (11).

Immunocytochemical analysis. Cultured cells were washed twice with PBS(-), fixed and rendered permeable in 1:1 acetone: methanol solution for 10 min at -20°C. Prior to the primary antibody reaction, cells were covered with blocking solution [5% bovine serum albumin in PBS(-)] for 10 min to block non-specific antibody binding. After the cells were incubated with a rabbit polyclonal antibody to human MMS22L (generated to synthesized peptide MMS22L; please see above) or a mouse monoclonal antibody to human NFKBIL2 (Abnova), the Alexa Fluor 488-labelled donkey anti-rabbit secondary antibody (Molecular Probes) or Alexa Fluor 594-labbelled donkey anti-mouse secondary antibody (Molecular Probes) was added to detect endogenous MMS22L or NFKBIL2, individually. Nuclei were stained with 4',6-diamidino-2-phenylindole (DAPI). The antibody-stained cells were viewed with a laser-confocal microscope (TSC SP2 AOBS; Leica Microsystems).

RNA interference assay. Two independent siRNA oligonucleotides against *MMS22L* were designed using the *MMS22L* sequences (GenBank accession no: NM198468). Each siRNA (600 pM) was transfected into two NSCLC cell lines, LC319 and A549 or a cervical cancer cell line HeLa using 30 μl of lipofectamine 2,000 (Invitrogen) following the manufacturer's protocol. The transfected cells were cultured for seven days. Cell numbers and viability were measured by Giemsa staining and 3-(4,5-dimethylthiazol-2-yl)-2,5-diphenyltetrazolium bromide (MTT) assay in triplicate (cell counting kit-8 solution; Dojindo Laboratories). The siRNA sequences used were as follows: control-1 (si-LUC: luciferase gene from *Photinus pyralis*), 5'-CGUACGCGGAAUACUUCGA-3'; control-2 (CNT: On-TARGETplus siControl non-targeting siRNAs of a pool of four oligosnucleotides: 5'-UGGUUUACAUGUCGACUAA-3'; 5'-UGGUUUACAUGUUUUCUGA-3'; 5'-UGGUUUACAUG UUUUCCUA-3'; and 5'-UGGUUUACAUGUUGU GUGA-3'); siRNA-MMS22L-#1 (si-MMS22L-#1: 5'-CCGCCAAUAUCA UCUCUAAUU-3'); siRNA-MMS22L-#2 (si-MMS22L-#2: 5'-GAA CCUGCAAUACAUGGUAUU-3'). Downregulation of endogenous MMS22L expression in the cell lines by siRNAs for *MMS22L*, but not by controls, was confirmed by semiquantitative RT-PCR and western blot analyses.

Cell growth assay. COS-7 or HEK293 cells that express endogenous *MMS22L* at a very low level were transfected with mock or MMS22L-expressing vectors (pCAGGSn-3xFlag-MMS22L) using lipofectamine 2,000 transfection reagent (Roche). Transfected cells were incubated in the culture medium containing 0.8 mg/ml neomycin (Geneticin, Invitrogen) for 7 days. Expression of MMS22L as well as viability and colony numbers of cells were evaluated by western blot analysis, and MTT and colony-formation assays at day 7.

Flow cytometric analysis. Cells transfected with siRNA oligonucleotides against *MMS22L* or control siRNAs were plated at densities of $5x10^5$ per 60-mm dish. Cells were collected in PBS, and fixed in 70% cold ethanol for 30 min. After treatment with 100 μg/ml RNase (Sigma-Aldrich), the cells were stained with 50 μg/ml propidium iodide (Sigma-Aldrich) in PBS. Flow cytometric analysis was done on a Cell Lab Quanta SC (Beckman Coulter) and analyzed by CXP Analysis software (Beckman Coulter). The cells selected from at least 10,000 ungated cells were analyzed for DNA content.

Results

Expression of MMS22L in lung and esophageal cancers. We previously performed genome-wide expression profile analysis of 120 lung cancer cases using microarray consisting of 27,648 cDNAs or ESTs (5-10). Among the genes upregulated in lung and esophageal cancers, we identified *MMS22L* transcript to be frequently overexpressed in lung and esophageal cancers, and confirmed by semiquantitative RT-PCR experiments its elevated expression in all of eleven clinical lung cancers and in four clinical esophageal cancers, although its expression was not detectable in adjacent normal lung and esophagus tissues (Fig. 1a). We further confirmed by western blot analysis high levels of endogenous MMS22L protein in 11 of 12 lung cancer cell lines and in all of 9 esophageal cancer cell lines using anti-MMS22L antibody (Fig. 1b). Northern blot analysis of 16 normal tissues confirmed that *MMS22L* was hardly detectable in normal tissues except the testis (Fig. 1c).

Growth effect of MMS22L. To investigate the relevance of MMS22L to the growth and/or survival of cancer cells, we knocked down the expression of endogenous *MMS22L* in two lung cancer cell lines, LC319 and A549, by means of the RNAi technique using siRNA oligonucreotide for *MMS22L*. Semiquantitative RT-PCR experiments detected significant reduction of MMS22L expression in the cells transfected with siRNAs against *MMS22L* (si-#1 and si-#2), but not in those with control siRNAs (si-LUC and si-CNT) (Fig. 2a). Colony formation and MTT assays clearly demonstrated that the viability of lung cancer cells transfected with two effective siRNAs for *MMS22L* (si-#1 and si-#2) were reduced in correlation with the reduction of MMS22L expression level, implying essential role of MMS22L in the growth of cancer cells (Fig. 2b and c). Since our original gene expression profile database also revealed its high level of expression in clinical cervical cancers, we also knocked down the expression of *MMS22L* by siRNAs in a cervical cancer cell line, HeLa, and observed the growth suppressive effect by siRNAs for *MMS22L*.

To further examine the effect of MMS22L overexpression on the growth of mammalian cells, we transiently transfected plasmid designed to express Flag-tagged MMS22L (pCAGGSn-3xFlag-MMS22L) or mock plasmid into COS-7 or HEK293 cells that expressed endogenous MMS22L at very low level. The significant growth promoting effect was observed in the cells transfected with the MMS22L expressing vector compared to those transfected with the mock vector (Fig. 2d).

NFKBIL2 controls the nuclear localization and stability of MMS22L protein. To investigate the biological function of MMS22L protein, we screened MMS22L-interacting proteins in lung cancer cells using mass spectrometric analysis and identified the interaction between MMS22L and NFKBIL2 [nuclear factor of kappa (NFKB) light polypeptide gene enhancer in B-cells inhibitor-like 2]. Previous reports independently suggested the roles of MMS22L-NFKBIL2 interaction in genomic stability and DNA replication in immortalized cell lines (46-49), however, no study has indicated critical roles of activation of MMS22L and NFKBIL2 in clinical cancers and investigated their functional importance in carcinogenesis. Western blot analysis using cell lines derived from lung cancers and antibodies to MMS22L and NFKBIL2 revealed the co-expression of these two proteins (data not shown), suggesting some functional roles of their interaction in human carcinogenesis. Therefore, we next performed immunofluorescence analysis to determine the subcellular localization of endogenous MMS22L and NFKBIL2 in various cancer cell lines including A549, LC319 and HeLa cells, and found that endogenous MMS22L and NFKBIL2 proteins were mainly co-localized in the nucleus (representative data of HeLa cells was shown in Fig. 3a). To examine the importance of MMS22L-NFKBIL2 interaction in cellar localization of these proteins, we transiently co-expressed exogenous MMS22L and NFKBIL2 proteins using mammalian COS-7 or NIH3T3 cells that expressed these two proteins at very low levels. We found that exogenous MMS22L was mainly located in the cytoplasm and weakly in the nucleus of the cells in which exogenous NFKBIL2 protein was not introduced. However, the nuclear staining of MMS22L was significantly enhanced when both exogenous MMS22L and NFKBIL2 proteins were introduced in the cells (Fig. 3b). On the other hand, exogenous NFKBIL2 was mainly present in the nucleus of cells regardless to the presence or absence of exogenous MMS22L. In addition, we performed western blot analysis using fractionated cytoplasmic and nuclear lysates from COS-7 cells that were introduced exogenous MMS22L and NFKBIL2 proteins. When we transfected both MMS22L-Flag and NFKBIL2-HA expressing vectors, the amounts of nuclear MMS22L was significantly increased, compared with the cells transfected with MMS22L alone (Fig. 3c). Furthermore, we found that knockdown of endogenous MMS22L with siRNA for *MMS22L* (si-*MMS22L*) reduced NFKBIL2 protein level in lung cancer LC319 cells and that reduction of NFKBIL2 with si-NFKBIL2 reduced MMS22L levels and significantly suppressed cancer cell growth (Fig. 3d; data not shown). These data suggest that the expression of NFKBIL2 is likely to promote nuclear localization and stability of MMS22L protein, and a complex including these two proteins could coordinately play pivotal roles in cell growth and/or survival.

C-terminal portion of NFKIL2 protein is crucial for binding to MMS22L protein. To examine whether the MMS22L-NFKBIL2 protein complex may play important roles in carcinogenesis, we subsequently constructed various plasmids expressing partial MMS22L proteins with Flag tag or partial NFKBIL2 proteins with HA tag, and transfected them into COS-7 cells (data not shown). Immunoprecipitation and western blotting assays using antibodies to Flag- or HA-tags revealed that an N-terminal portion of MMS22L protein (M1; codon 1-414) could bind to a C-terminal region of NFKBIL2 (N3; codon

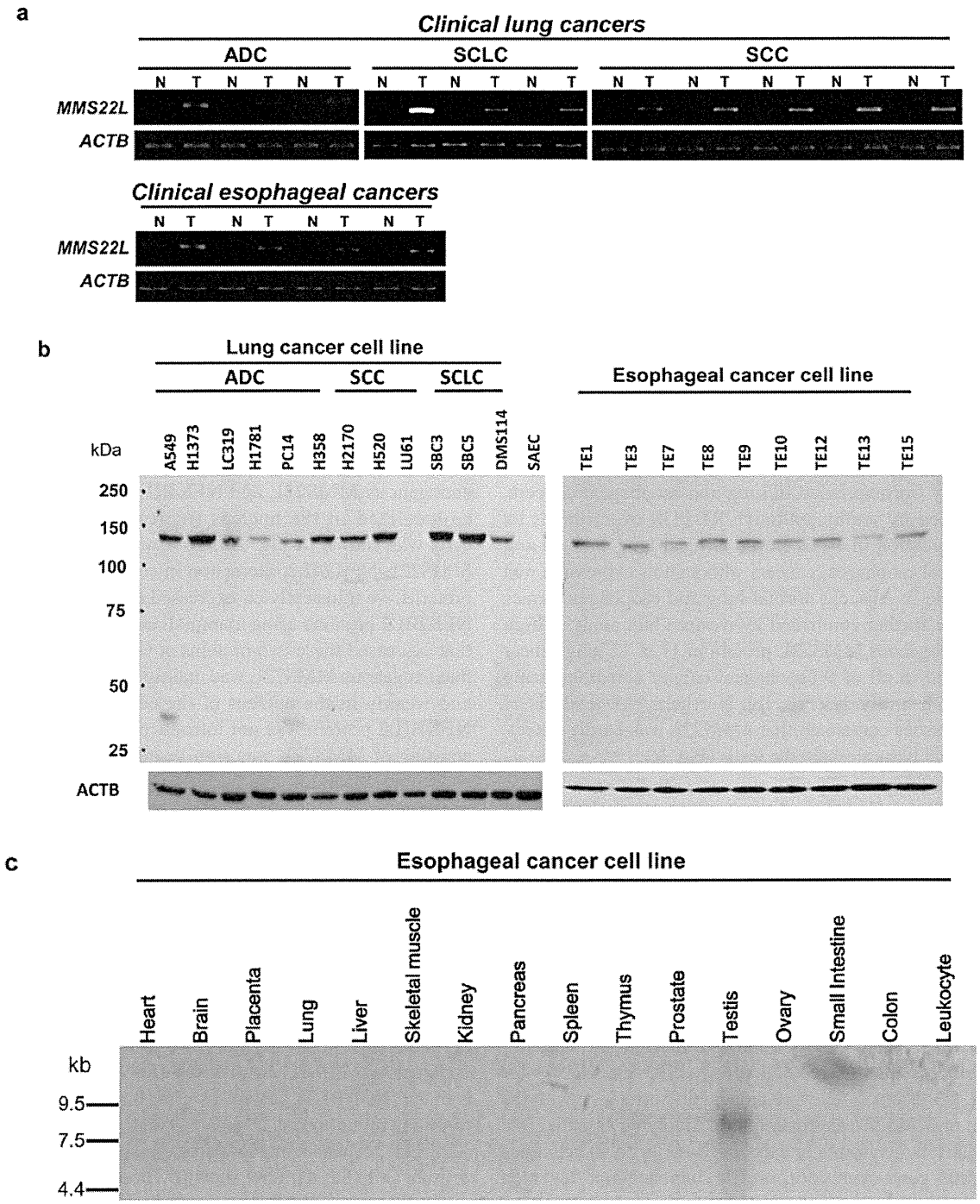

Figure 1. Expression of MMS22L in lung and esophageal cancers and normal tissues. (a) Expression of *MMS22L* gene in (T) lung and esophageal cancer tissues and (N) adjacent normal lung and esophagus tissues, detected by semiquantitative RT-PCR. (b) Expression of MMS22L protein in lung and esophageal cancer cell lines, detected by western blot analysis. (c) Northern blot analysis of the *MMS22L* transcript in 16 normal human tissues.

823-1244) (Fig. 4a). Because immunocytochemical analysis revealed that nuclear localization of MMS22L protein appeared to require the presence of NFKIL2 protein in the nucleus (Fig. 3b), we subsequently investigated which part of NFKBIL2 protein is essential for subcellular localization of MMS22L protein in cultured cells. Plasmids expressing partial proteins of NFKBIL2 were co-transfected with full-length MMS22L expression vector into COS-7 cells. Interestingly, N-terminal (N1; codon 1-450) and central part (N2; codon 403-836) of NFKBIL2 proteins could be localized in the nucleus, while aggregated MMS22L protein was mainly located in the cytoplasm of the same cells (Fig. 4b). It is concordant with the data that these two partial proteins (N1 and N2) could not bind to MMS22L protein as indicated by immunoprecipitation analyses. In contrast, MMS22L protein and C-terminal part of NFKBIL2 protein (N3; codon 823-1244) that could bind to

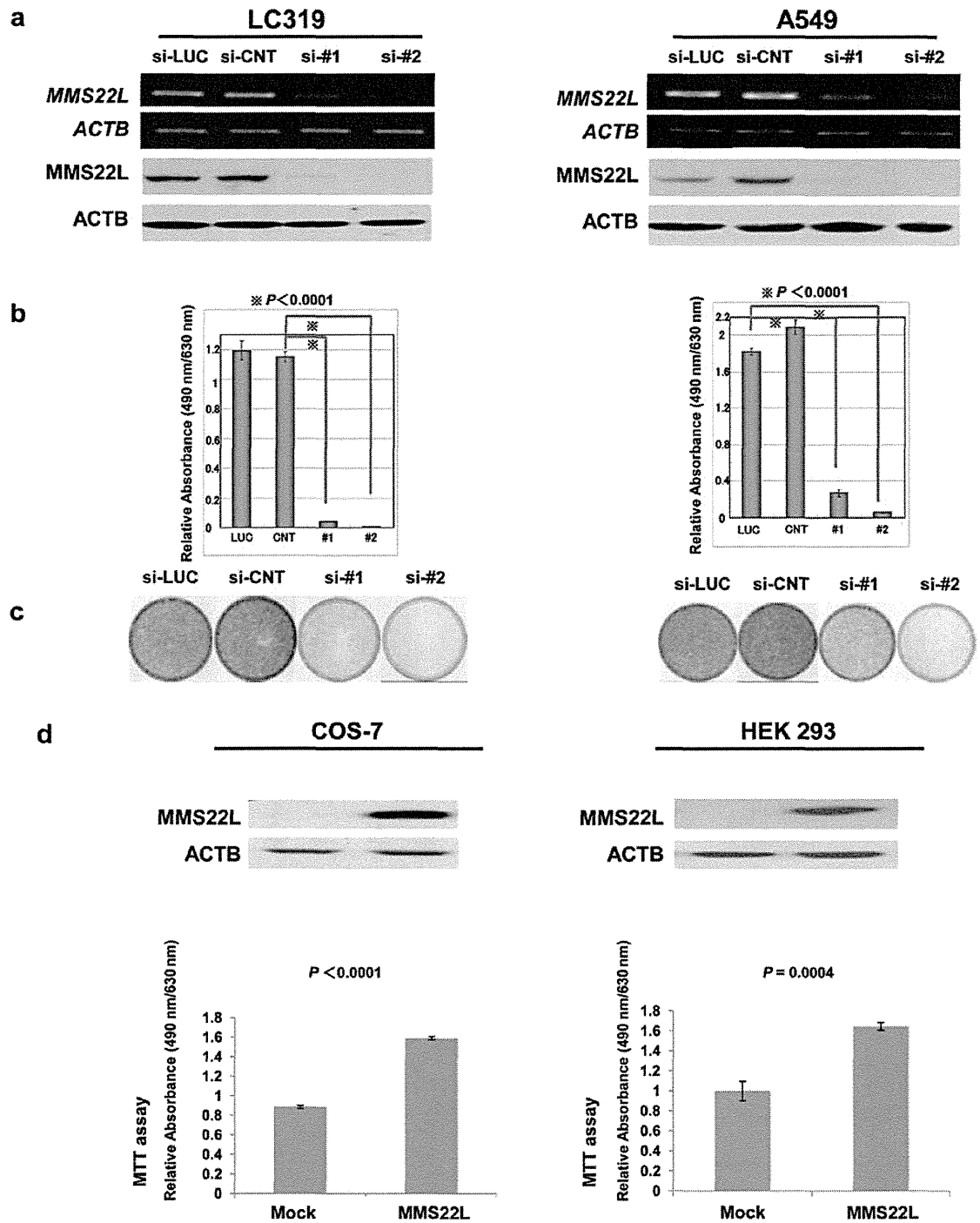

Figure 2. Growth effect of MMS22L. (a) Knockdown of MMS22L expression in lung cancer cell lines, LC319 and A549 by specific siRNA oligonucleotides for *MMS22L* (si-#1 and si-#2) or control siRNAs (si-LUC and si-CNT), confirmed by semiquantitative RT-PCR and western blot analyses. (b) Viability of A549 and LC319 cells evaluated by MTT assay in response to the siRNAs. All assays were performed in triplicate wells at three independent times. (c) Colony formation assays using LC319 and A549 cells transfected with the siRNAs. (d) Enhanced growth promoting activity of COS-7 and HEK293 cells transfected with mock or MMS22L expressing vectors as quantified by MTT assay at 7 days after transfection.

MMS22L protein were mainly localized in the cytoplasm of the cells (Fig. 4b). The data indicate that N-terminal (N1; codon 1-450) and central (N2; codon 403-836) parts of NFKBIL2 are more important for nuclear localization of NFKBIL2, while its C-terminal part (N3; codon 823-1244) is essential for binding to MMS22L.

Dominant negative growth suppressive effect of partial NFKBIL2 protein including MMS22L-binding site. According to the data above, we hypothesized that if nuclear localization of MMS22L protein is important for cancer cells growth, reduction of MMS22L protein in the nucleus by inhibiting the interaction between MMS22L and NFKBIL2 could suppress the cancer cell

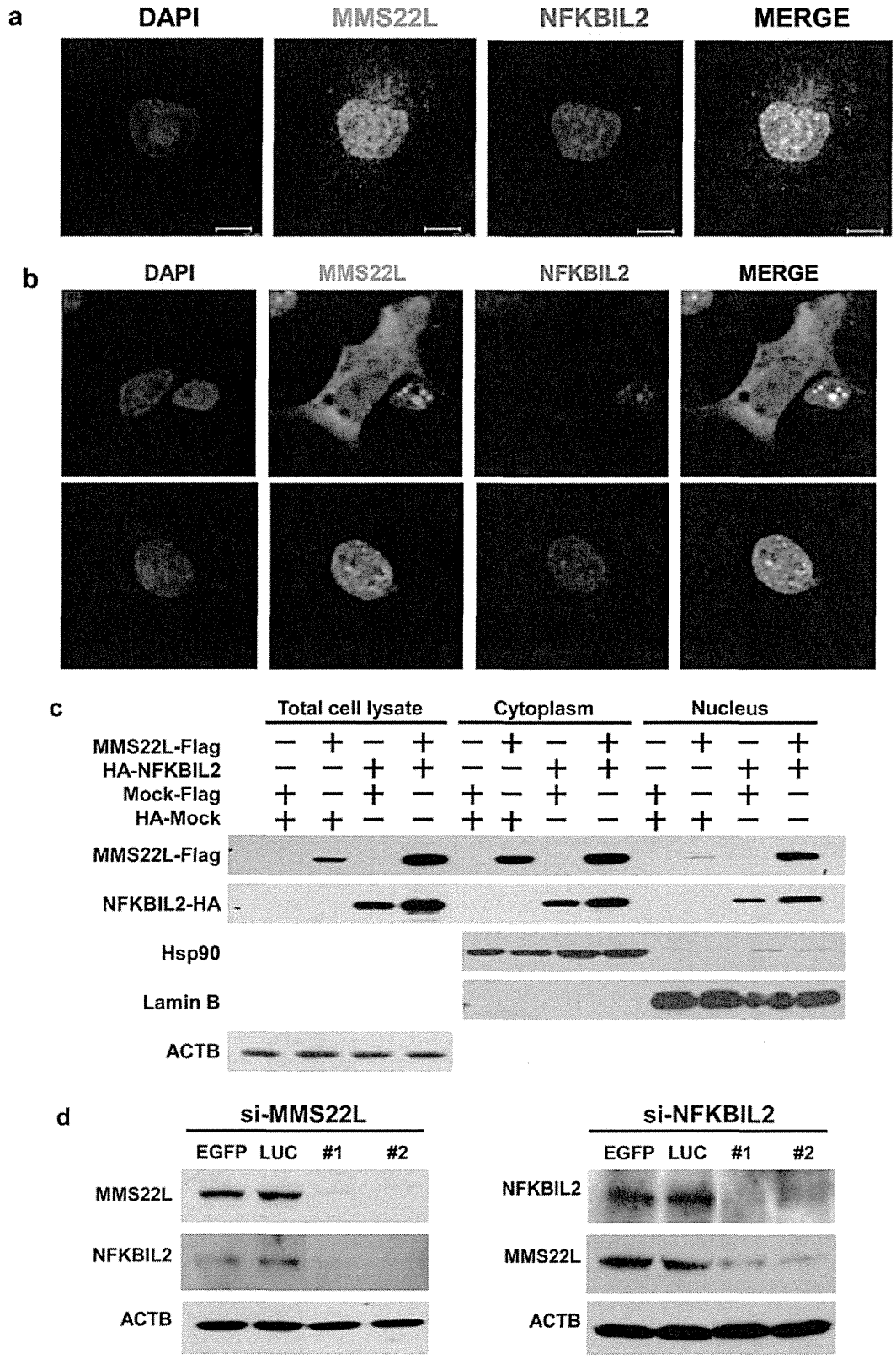

Figure 3. Nuclear localization and stability of MMS22L and its interacting protein of NFKBIL2 in cultured cells. (a) Subcellular localization of endogenous MMS22L and NFKBIL2 proteins in HeLa cells. The cells were stained with a rabbit polyclonal anti-MMS22L antibody (green); mouse polyclonal anti-NFKBIL2 (red) and with DAPI (blue). (b) Subcellular localization of MMS22L in the presence or absence of NFKBIL2 protein. COS-7 cells were co-transfected with Flag-tagged MMS22L- and HA-tagged NFKBIL2-expression vectors. MMS22L protein was stained with anti-Flag M2 antibody (green); NFKBIL2 with anti-HA (red) and nucleus with DAPI (blue). (c) Western blot analysis using cytoplasmic and nuclear fraction of COS-7 cells which were co-transfected with MMS22L- and NFKBIL2- expression vectors. MMS22L and NFKBIL2 proteins were detected using anti-Fag-M2 antibody and/or anti-HA (3F10) antibody. (d) Knockdown of MMS22L or NFKBIL2 protein expression with si-*MMS22L* or si-*NFKBIL2* oligonucleotides. The expression of endogenous MMS22L and NFKBIL2 proteins were detected by western blot analysis using anti-MMS22L antibody and anti-NFKBIL2 antibody.

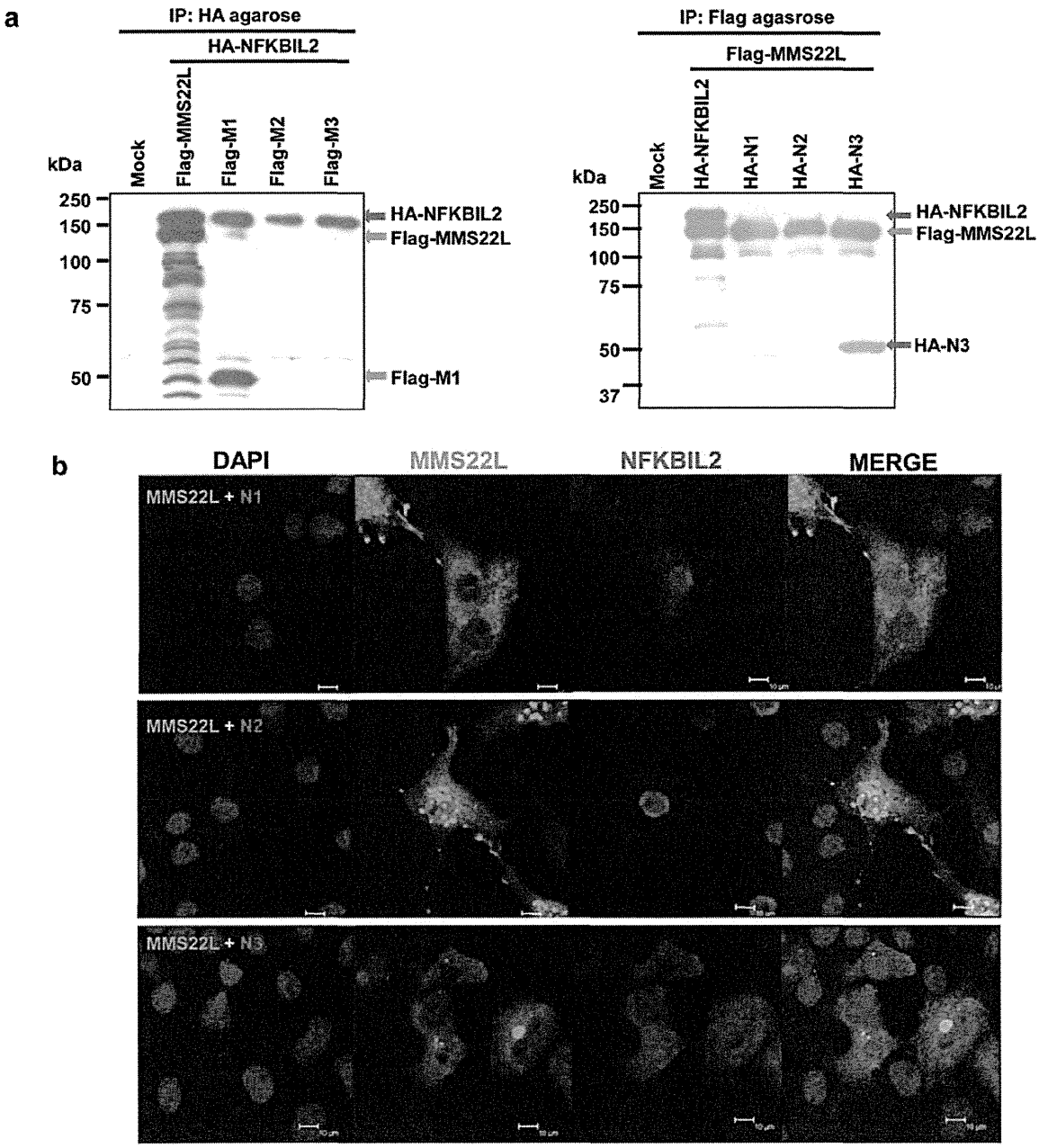

Figure 4. C-terminal portion of NFKIL2 protein is crucial for binding to MMS22L protein. (a) Binding between MMS22L and NFKBIL2 proteins detected using Flag- or HA-agarose and COS-7 cells co-transfected with full-length/partial MMS22L-Flag and full-length/partial NFKBIL2-HA proteins. (b) Subcellular localization of full-length MMS22L and three partial NFKBIL2 proteins. COS-7 cells were co-transfected with full-length MMS22L and partial NFKBIL2-expression vectors (N1-N3). MMS22L protein was stained with anti-Flag M2 antibody (green); NFKBIL2 with anti-HA antibody (red) and nucleus with DAPI (blue).

growth. To examine whether exogenous expression of partial N3 protein can inhibit the MMS22L-NFKBIL2 interaction and cell growth, we co-transfected full-length MMS22L and either of full-/partial-length NFKBIL2 expressing vectors (N1, N2 or N3) into HEK293 cells, and found that the amount of exogenous full-length NFKBIL2 protein that binds to exogenous MMS22L was significantly decreased after introduction of the partial N3 protein, as demonstrated by immunoprecipitation assays, while it was not changed in the cells transfected with N1 or N2 vectors (Fig. 5a). To investigate the functional significance of the interaction between MMS22L and NFKBIL2 for growth of cancer cells, we transfected either of vectors expressing partial NFKBIL2 proteins or mock vectors into two cancer cell lines, HeLa and LC319, which highly expressed both endogenous MMS22L and NFKBIL2 proteins and lung fibroblast CCDlu-19 cells in which MMS22L expression was hardly detectable. Expectedly, exogenous expression of the C-terminal portion of NFKIL2 protein (N3) reduced the levels of MMS22L protein in the nucleus and inhibited the growth of HeLa and LC319 cells as measured by MTT assay, while it did not affect the growth of MMS22L-negative CCDLu-19 cells (Figs. 5b-d). Our findings imply that inhibition of the interaction between the MMS22L